WIND RESILIENCE IN OVERWINTERING MONARCH BUTTERFLIES: AN EMPIRICAL TEST OF THE MICROCLIMATE HYPOTHESIS

A Thesis

presented to

the Faculty of California Polytechnic State University,

San Luis Obispo

In Partial Fulfillment

of the Requirements for the Degree

Master of Science in Biological Sciences

by

Kyle Nessen

December 2025

© 2025
Kyle Nessen
ALL RIGHTS RESERVED

COMMITTEE MEMBERSHIP

TITLE: Wind Resilience in Overwintering Monarch Butterflies: An Empirical Test of the Microclimate Hypothesis

AUTHOR: Kyle Nessen

DATE SUBMITTED: December 2025

COMMITTEE CHAIR: Dr. Matt Ritter, Ph.D.
Professor of Biology

COMMITTEE MEMBER: Dr. Francis Villablanca, Ph.D.
Professor Emeritus of Biology

COMMITTEE MEMBER: Dr. Jenn Yost, Ph.D.
Associate Professor of Biology

ABSTRACT

Wind Resilience in Overwintering Monarch Butterflies: An Empirical Test of the Microclimate Hypothesis

Kyle Nessen

The western monarch butterfly (*Danaus plexippus*) population has declined by over 99% since the 1980s, making conservation of overwintering habitat along California's coast a management priority. For three decades, habitat management has followed the Disruptive Wind Hypothesis, which posits that wind speeds exceeding 2 m/s disrupt butterfly clusters and cause roost abandonment. This threshold has had substantial influence on restoration practices, despite lacking direct empirical validation.

This study provides the first experimental test of wind effects on overwintering monarch clusters. We deployed cameras and wind sensors at two sites on Vandenberg Space Force Base during the 2023-2024 overwintering season, collecting 1,894 paired observations at 30-minute intervals across 78 days. Time-lapse photography documented butterfly abundance while wind sensors at roost height recorded wind conditions.

Linear regression analysis revealed no significant relationship between wind speed and changes in cluster size at either 30-minute or daily timescales ($R^2 = 0.002$, p = 0.073 and $R^2 = 0.013$, p = 0.252, respectively). Every day with butterflies present experienced wind speeds exceeding the 2 m/s threshold, yet clusters persisted throughout the monitoring period. Generalized additive mixed models identified temperature, time of day, and an interaction between wind and sunlight as factors influencing cluster behavior ($p < 0.001$), but wind alone showed no independent effect. When butterflies remained in shade, wind speed had no effect on cluster behavior across the entire observed range (0 to 12.4 m/s). Effects appeared only when butterflies occupied sunlit positions, suggesting that thermoregulation may be a primary driver of clustering behavior.

Our findings challenge fundamental assumptions in monarch habitat management. The absence of wind disruption indicates that monarchs may be more resilient to environmental variation than previously believed, with suitable habitat potentially more

extensive than currently recognized. Conservation efforts should continue promoting healthy groves while reconsidering strict wind-based management requirements. Future research should investigate canopy structure and resulting light patterns that monarchs may select when choosing roost sites. As western monarch populations continue to face historic lows, evidence-based understanding of overwintering ecology becomes essential for effective conservation.

Keywords: Monarch butterfly, overwintering behavior, wind effects, microclimate, Vandenberg Space Force Base, time-lapse photography, generalized additive mixed models, behavioral ecology, California.

ACKNOWLEDGMENTS

I would like to express my sincere gratitude to my committee for their mentorship, support, and advocacy throughout this thesis. In particular, I thank Dr. Francis Villablanca, who gave his time generously by providing invaluable mentorship on the scientific process.

This research benefited immensely from the "Super Study" group, whose many meetings provided excellent feedback and insights at all stages of my project. I thank Emma Pelton, Peter Ibsen, Jay Diffendorfer, Jessica Griffiths, Ashley Fisher, Sara Cuadra-Vargas, Charis van der Heide, Stephanie Little, and Ray Danner for their collaboration and expertise. Emma Pelton was instrumental in gathering these experts together, securing funding for my project, and initially seeding the idea for this study. Peter Ibsen and Jay Diffendorfer at USGS provided crucial funding support and valuable feedback throughout. Jessica Griffiths was instrumental in securing site access at Vandenberg Space Force Base, helping select study sites, and interpreting results. Ashley Fisher provided extensive discussions about monarch ecology and field assistance.

I am deeply grateful to my undergraduate research assistants who conducted all photo labeling and provided essential field assistance: Skyler Meinholz, Vincent Rios, Emery Doornbos, and Kevin Untalan. Their dedication and hard work made this research possible.

I thank LynneDee Althouse, Dan Meade, Stu Weiss, and Charis van der Heide, along with the many wonderful people at Althouse and Meade, Inc., for their collaboration and mentorship during my early monarch work, which laid the foundation for this thesis.

I thank my family and friends for their unwavering support and encouragement as I changed careers to pursue this project, especially my wife, Emily Nessen, whose patience and encouragement sustained me throughout.

This research was made possible through generous funding from The Xerces Society for Invertebrate Conservation, US Forest Service International Programs, Department

of Defense Legacy Resource Management Program, and the United States Geological Survey.

Finally, this work is dedicated to the memory of Dan Meade, who revealed the fascinating mysteries of monarch butterflies to me and provided the rare freedom to explore them. His patience, generosity, and belief in my ideas helped make this research possible.

TABLE OF CONTENTS

LIST OF TABLES

LIST OF FIGURES

Chapter 1

INTRODUCTION

The distribution and survival of invertebrate species are governed by a complex interplay of biotic and abiotic factors. While biotic interactions influence community assembly in part through predation, competition, and parasitism (Blois-Heulin, Crowley, Arrington, & Johnson, 1990; Lafferty & Shaw, 2013; Miller-ter Kuile, Apigo, Bui, et al., 2022), abiotic conditions often set the fundamental limits determining where invertebrates can persist. Temperature constrains invertebrate physiology across all latitudes, from Antarctic midges (*Belgica antarctica*) that survive freeze-thaw cycles through cryoprotective dehydration (Everatt, Convey, Bale, et al., 2015), to desert land snails (*Sphincterochila boissieri*) that tolerate 55°C through metabolic downregulation (Schweizer, Triebskorn, & Köhler, 2019). Rising temperatures directly increase metabolic rates and respiratory water loss, creating compound stress that limits activity windows (Chown, Sørensen, & Terblanche, 2011). Solar radiation drives both direct physiological impacts and behavioral responses. Army ants demonstrate habitat-specific evolution of thermal maxima tied to insolation exposure (Baudier, D'Amelio, Malhotra, et al., 2018), while terrestrial gastropods climb vertical surfaces to escape ground-level heat and evolve reflective pigmentation in exposed populations (Schweizer, Triebskorn, & Köhler, 2019).

Wind influences invertebrate behavior and ecology through diverse mechanisms that vary across species, exhibiting remarkably specific wind detection thresholds and behavioral responses. Cockroaches (*Periplaneta americana*) perceive air currents as low as 0.015–0.03 m/s, demonstrating predictable orientation shifts from upwind movement at low velocities to downwind escape at higher speeds (Bell & Kramer, 1979).

Mosquito flight activity shows sensitivity to even light winds, with trap catches declining 75% when wind speeds approach their normal flight velocity of 1.0 m/s, effectively grounding entire populations (Bidlingmayer, Day, & Evans, 1995). Some species exploit wind for dispersal through specific behavioral triggers, such as spiders exhibiting stereotypic 'tiptoe' behavior to initiate ballooning when wind conditions permit controlled trajectories (Bonte & Lens, 2007). Others respond to wind as an environmental stressor requiring active avoidance. Herbivorous larvae like the mad hatterpillar (*Uraba lugens*) treat moderate winds of 3 m/s as disturbance cues, triggering increased movement to stable microsites on branches and behavioral shifts to leeward sides and abaxial leaf surfaces for protection (Leonard, McArthur, & Hochuli, 2016). Underlying many of these behavioral responses are the fundamental thermal and hydric effects of wind, as convective cooling from air movement significantly alters heat and water exchange between organisms and their environment, particularly when interacting with solar radiation (Riddell & Porter, 2025).

Beyond direct physical effects, invertebrates detect wind through indirect sensory pathways. The Namib desert beetle *Lepidochora discoidalis* perceives substrate vibrations when winds exceeding 5 m/s lift sand grains, using these cues to time surface foraging when detritus becomes concentrated (Hanrahan & and Kirchner, 1997). The katydid *Copiphora brevirostris* adjusts vibratory communication to avoid wind-induced noise, concentrating signaling between 2:00 and 5:00 AM when winds are calmest and exploiting short-term lulls during gusty periods (Velilla, Muñoz, Quiroga, et al., 2020). This complexity in wind-organism interactions becomes particularly evident when examining species that must navigate multiple life stages with different environmental exposures.

The monarch butterfly (*Danaus plexippus*) offers an exceptional system for studying how abiotic factors, particularly wind, shape invertebrate ecology through its remark-

able multi-generational migration. North American monarchs complete an annual cycle that links vast northern breeding ranges with small, highly specific overwintering sites (L. Brower, 1995; S. Jepsen, Schweitzer, Young, et al., 2015; Solensky, 2004). North America is home to two populations of monarchs separated by the Rocky Mountains: a larger Eastern population and a Western population (Cockrell, Malcolm, & Brower, 1993; Freedman, de Roode, Forister, et al., 2021; S. Jepsen, Schweitzer, Young, et al., 2015). In spring, the overwintered generation migrates northward from their wintering sites to the southern United States where they breed and die. Their offspring and subsequent generations continue breeding and progressively colonizing northward throughout spring and summer, with multiple short-lived generations (2–5 weeks) breeding across an expanding range (Cockrell, Malcolm, & Brower, 1993; Zalucki, 1982). Females lay eggs exclusively on milkweed (*Asclepias* spp.), the larval host plant. This successive breeding and northward expansion builds the population through three to four generations, until late summer when environmental cues such as shortening day length and cooling temperatures trigger the emergence of the migratory generation (Barker & Herman, 1976; Goehring & Oberhauser, 2002; Herman & Tatar, 2001; Reppert & de Roode, 2018). These migratory adults exhibit a unique phenotype: they enter a state of reproductive diapause (suspended reproduction) and possess elongated wings suited for long-distance travel (Barker & Herman, 1976; Tuskes & Brower, 1978; Yang, Ostrovsky, Rogers, & Welker, 2016).

The fall migration begins as these long-lived adults (6–8 months) orient themselves southward, flying up to thousands of kilometers, nectaring at flowers along their route to build the lipid reserves needed for the long overwintering period (Chaplin & Wells, 1982; Herman & Tatar, 2001; Urquhart & Urquhart, 1978). Navigational feats are guided by a sophisticated system that includes a time-compensated sun compass residing in the antennae, allowing them to maintain direction throughout the day (Mouritsen & Frost, 2002; Nguyen, Beetz, Merlin, & el Jundi, 2021). Eastern

monarchs travel to the high-altitude oyamel fir (*Abies religiosa*) forests in central Mexico, while the Western population migrates to overwintering groves located along the Pacific coast of California (L. Brower, 1995; Urquhart & Urquhart, 1978).

The overwintering period, lasting roughly from mid-October through mid-March, represents an important phase of the annual migration where the entire North American population concentrates into remarkably small, forested areas (S. J. Jepsen & Black, 2015; Solensky, 2004; Vidal & Rendón-Salinas, 2014). During these months, monarchs must survive exclusively on lipid reserves accumulated during the autumn migration while maintaining precise thermoregulatory balance (Chaplin & Wells, 1982; Masters, Malcolm, & Brower, 1988). As ectotherms, monarchs face a fundamental trade-off: they must maintain body temperatures cool enough to conserve energy through metabolic suppression, yet warm enough to permit essential daily movement (Alonso-Mejia & Arellano-Guillermo, 1992; Chaplin & Wells, 1982; Kammer, 1970; Masters, Malcolm, & Brower, 1988). The flight threshold, established at 12.7-16.0°C for Eastern populations, represents the minimum thoracic temperature required for powered flight (Masters, Malcolm, & Brower, 1988). Below this threshold, monarchs employ behavioral thermoregulation through dorsal basking, which can elevate body temperature to flight capability within 30 seconds of sun exposure, or through energetically costly shivering that consumes energy 25 times faster than resting (Masters, Malcolm, & Brower, 1988). Conversely, temperatures above 20°C risk terminating reproductive diapause and triggering premature remigration, while direct sun exposure can rapidly elevate thoracic temperatures to 33.6°C, forcing butterflies to adopt sun-minimizing postures or engage in heat-dissipating flights (Barker & Herman, 1976). This delicate energetic balance means that monarchs selecting overwintering sites must find locations that minimize both freezing risk and elevated metabolic expenditure (Alonso-Mejia & Arellano-Guillermo, 1992; Calvert, Zuchowski, & Brower, 1983; Masters, Malcolm, & Brower, 1988).

Building on early studies from Mexican overwintering sites that identified abiotic factors limiting butterfly survival, Leong proposed the microclimate hypothesis for western monarchs overwintering in California (K. L. H. Leong, 1990). This hypothesis posited that monarchs select clustering locations within groves based on a measurable microenvironmental envelope characterized by four key parameters: wind protection below 2 m/s (5 mph) to prevent cluster disruption, cool temperatures maintaining reproductive diapause while avoiding freezing mortality, dappled sunlight enabling behavioral thermoregulation, and high humidity with accessible moisture to prevent desiccation (K. L. H. Leong, 1990; K. L. Leong, Frey, Brenner, et al., 1991). Wind emerged as particularly critical in this framework, though these conclusions derived from correlational measurements rather than direct behavioral observations. Leong's initial studies measured wind speeds at trees with and without butterfly clusters, while noting that "during winter storms, the butterflies clustered on those few trees that offered the greatest protection against winds of 2 m/s or greater" (K. L. H. Leong, 1990), though the highest wind speed measured in this study was 1.66 m/s. Based on these correlational patterns, Leong reported that "butterflies cluster in areas of the grove that offer exposure to filtered sunlight and shelter from strong wind movement" (K. L. Leong, Frey, Brenner, et al., 1991). In later publications, Leong described increasingly dramatic wind effects through anecdotal observations, noting that "roosting butterflies were blown from their clusters or dislodged by excessive branch movements (shaking) caused by winds exceeding 2 m/s" and that "upon dislodgment, the butterflies flew to and resettled on foliage of trees that offered better shelter from strong winds" (K. L. H. Leong, 1999). When storm winds coincided with cold morning temperatures below 15°C, "the dislodged butterflies would be blown to the ground and remain there until temperatures reached flight threshold," with "butterflies littering the ground at the base of roosting trees" commonly observed after winter storms (K. L. H. Leong, 1999). Despite originating from correlational

field measurements and anecdotal observations, this hypothesis gained widespread acceptance and directly informed management guidelines at multiple levels. Leong's 2016 synthesis for California Department of Fish and Wildlife formally established that "winds $\geq$ 2 m/s are disruptive to the aggregating butterflies by blowing them from their roosting branches or dislodging them by shaking the branches," and that when subjected to such winds above flight threshold, butterflies "either flew to a more sheltered area of the grove or, if no refuge area was available, abandoned the grove temporarily or for the remainder of the season" (K. L. H. Leong, 2016). The microclimate hypothesis thus dictated that successful overwintering sites must consistently exhibit this specific suite of conditions, particularly wind protection from $\geq$ 2 m/s wind speed, implying that these abiotic parameters should guide habitat restoration efforts, a principle now widely adopted in monarch conservation plans (Althouse & Meade, Inc. & Creekside Science, 2023; S. Jepsen, Pelton, Black, et al., 2017; E. Pelton, 2020; Weiss & Rich, 2008; Xerces Society, 2016).

However, empirical testing has gradually dismantled the microclimate hypothesis's core assumption of a uniform environmental envelope. When researchers tested whether monarchs select for consistent microclimatic attributes across groves, they found that the realized microclimate varied significantly with latitude and local geography (Saniee & Villablanca, 2022). Temperature responses proved more complex than originally proposed, with monarchs avoiding freezing temperatures but selecting the warmest of cold temperatures available at their latitude (Fisher, Saniee, Van der Heide, et al., 2018). Humidity requirements showed geographic variability rather than consistency (Saniee & Villablanca, 2022). Of the four original parameters, only light exposure showed potential support as a unifying factor, with successful overwintering sites exhibiting consistent patterns of canopy openness (Saniee & Villablanca, 2022; Weiss, Rich, Murphy, et al., 1991). This geographic variability in microclimate preferences, where selection occurs hierarchically across multiple spatial scales

rather than for a single environmental envelope, fundamentally contradicts Leong's original hypothesis (Fisher, Saniee, Van der Heide, et al., 2018; Saniee & Villablanca, 2022). The gradual rejection of the uniform microclimate hypothesis through empirical testing suggests that monarch habitat selection may be driven by physiological and energetic constraints that vary with local environmental conditions rather than by a rigid set of universal requirements.

Among the four parameters of Leong's microclimate hypothesis, wind disruption stands apart as the only major component that has never undergone direct empirical testing of butterfly behavioral responses. Despite widespread adoption of the 2 m/s wind protection threshold in restoration efforts, no study has established causal relationships between wind exposure and butterfly behavior (Althouse & Meade, Inc. & Creekside Science, 2023; S. Jepsen, Pelton, Black, et al., 2017; K. L. H. Leong, 2016; U.S. Fish and Wildlife Service, 2024; Weiss, 2018; Xerces Society, 2018). Leong's methodology of comparing wind measurements between occupied and unoccupied trees provided only correlational evidence, never directly testing butterfly responses to wind exposure or distinguishing whether butterflies actively avoid wind or whether wind simply correlates with other unmeasured variables.

The absence of empirical testing for the wind disruption component of the microclimate hypothesis becomes critically important given the catastrophic decline of western monarch populations. Between the 1980s and mid-2010s, populations collapsed by approximately 97% (Schultz, Brown, Pelton, & Crone, 2017), with population viability analyses revealing a 72% quasi-extinction risk within 20 years (Schultz, Brown, Pelton, & Crone, 2017). The winter 2018 to 2019 count recorded fewer than 30,000 monarchs, a single-year drop of 86%, representing over 99% decline from 1980s abundance (E. M. Pelton, Schultz, Jepsen, et al., 2019). The situation reached its most critical state in 2020 when the Western Monarch Thanksgiving Count documented

only 1,901 butterflies, the lowest number ever recorded (Xerces Society, 2025a). While populations showed some recovery in subsequent years, the 2024 to 2025 count of just 9,119 butterflies represents the second-lowest count on record, demonstrating the population's continued precarity (Xerces Society, 2025a). These dramatic declines result from multiple interacting stressors including breeding habitat loss, pesticide exposure, climate change, and critically, the loss and degradation of overwintering habitat (Crone, Pelton, Brown, et al., 2019; E. M. Pelton, Schultz, Jepsen, et al., 2019). Evidence increasingly suggests that the overwintering stage represents the most limiting phase of the monarch's annual cycle, with population declines concentrated during winter and early spring periods (Marini & Zalucki, 2017; E. M. Pelton, Schultz, Jepsen, et al., 2019). California's coastal overwintering groves, where the entire western population concentrates into small forested areas from October through March, have thus emerged as the focal point of conservation priorities. Yet management of these critical sites continues to rely on the untested wind disruption component of the microclimate hypothesis, with restoration efforts investing millions of conservation dollars based on the presumed necessity of maintaining wind speeds below 2 m/s (Althouse & Meade, Inc. & Creekside Science, 2023; The Monarch Press, 2019).

Testing the wind disruption component requires addressing a fundamental methodological challenge: isolating wind effects from confounding environmental variables that naturally covary in field settings. Solar radiation can trigger butterfly departures through direct heating, enabling flight when ambient temperatures remain below thermal thresholds (Kammer, 1970; Masters, Malcolm, & Brower, 1988). Temperature independently influences activity patterns, with monarchs exhibiting predictable responses as temperatures approach and exceed flight thresholds (Barker & Herman, 1976). Time of day creates inherent activity rhythms related to sun angle and thermal conditions (Mouritsen & Frost, 2002). Furthermore, wind itself is multidimensional, characterized not only by average speed but also by gustiness and variability (Nathan,

Sapir, Trakhtenbrot, et al., 2005) that could differentially affect butterfly behavior. A rigorous test must therefore control for these confounding factors while examining multiple aspects of wind exposure, including both maximum wind speeds and duration above the proposed 2 m/s threshold. With western monarch populations facing potential extinction and limited conservation resources available, the need for empirically validated management strategies has never been more urgent.

This study provides the first direct empirical test of whether wind disrupts overwintering monarch butterflies. Our primary objective was to evaluate the 2 m/s wind disruption threshold that has guided over three decades of conservation practice.

First, we hypothesized that wind, alongside other environmental factors, predicts butterfly abundance at overwintering clusters. If true, we predict that wind will emerge as a significant predictor of abundance changes, with monarch abundance decreasing when exposed to higher wind speeds.

Second, we hypothesized that wind becomes disruptive above a specific threshold of 2 m/s. If this threshold represents a meaningful biological boundary, we predict that monarch abundance will decline at roosts experiencing winds exceeding 2 m/s.

Third, we hypothesized that wind's disruptive effects scale with intensity. If disruption increases with wind speed, we predict proportionally greater decreases in monarch abundance as wind speeds rise above the threshold.

Finally, we hypothesized that experiencing disruptive winds affects monarch site fidelity. If wind disruption influences future roost selection, we predict decreased site fidelity manifested as sustained abundance reductions at wind-disturbed roosts compared to pre-disturbance levels.

Chapter 2

MATERIALS AND METHODS

2.1 Study Site

Site selection followed a systematic filtering process driven by project requirements and practical constraints. The study was supported by a federal grant that mandated research be conducted on federal lands. We selected Vandenberg Space Force Base (VSFB, 34.7398°N, 120.5725°W) in Santa Barbara County, California, based on several key advantages: mild winters with infrequent frost events, extensive historical plantings of blue gum eucalyptus (*Eucalyptus globulus*) that have created suitable overwintering habitat throughout the installation, and restricted access that provided security for long-term equipment deployment. The military base contains thirty documented monarch overwintering groves, with several sites consistently ranking within the top 10% of population counts statewide over the past decade (Xerces Society, 2025b).

Working with the base's monarch conservation coordinator, we initially screened twelve locations from the thirty sites based on their documented capacity to support monarch aggregations and provide year-round access. This collaboration leveraged local expertise from managing Western Monarch Thanksgiving Count activities for multiple years (Xerces Society, 2025b). From these twelve candidate sites, we deployed monitoring equipment at ten unique locations across both study seasons: four sites during the 2023-2024 season and ten sites during the 2024-2025 season. However, due to low monarch populations during the 2023-2024 season and no observed

overwintering behavior in the 2024-2025 season, only two sites (Spring Canyon and UDMH) produced measurable butterfly clusters suitable for our study.

Spring Canyon (34.6315°N, 120.6182°W) represents the most productive and historically reliable overwintering site on VSFB. Located in South Base within 300 meters of Space Launch Complex 4, this approximately 2.0-hectare site consists entirely of mature blue gum eucalyptus trees reaching heights of approximately 40 meters. An unnamed perennial creek runs through the center of the grove, creating a riparian corridor that supports heterogeneous canopy structure with variable tree spacing and diverse understory vegetation. Surf Road, an infrequently used paved access road, bisects both the perennial creek and forest canopy.

The second site, UDMH site (34.6719°N, 120.5950°W), also located in South Base, comprises a 5.1-hectare eucalyptus grove planted in windrows adjacent to a waste treatment facility. The uniformly spaced trees maintain a largely clear understory with scattered low shrubs. Although only recently documented as an overwintering location in 2022, UDMH immediately emerged as a significant site, supporting over 6,000 monarchs during its initial 2022 count and ranking among the base's highest population sites.

2.2 Monitoring Strategy

Equipment deployment strategies differed between monitoring seasons to accommodate research objectives and field experience. During the 2023-2024 season, we employed two strategies: targeted deployments at sites with confirmed monarch presence, and anticipatory deployments at locations where monarchs were expected based on historical data but not currently observed. Targeted deployments concentrated at Spring Canyon and UDMH where active aggregations were documented throughout

the season. Anticipatory deployments occurred at four overwintering sites: additional locations within Spring Canyon and UDMH, plus SLC-6 and Tangair. In the 2024-2025 season, no monarchs were recorded at these anticipatory deployment sites; consequently, these data are excluded from analysis.

Building on insights from the 2023-2024 season, for the 2024-2025 season we modified our approach to establish monitoring stations at ten sites before monarch arrival, based on historical occurrence records compiled by the base conservation coordinator. This expanded spatial coverage aimed to capture greater environmental variation across potential overwintering sites. However, the 2024-2025 season coincided with historically low monarch abundance throughout California (Xerces Society, 2025b), resulting in no observed clustering behavior at any of the ten monitored locations. Consequently, our analysis focuses exclusively on data collected during the 2023-2024 season.

2.3 Field Equipment

To observe changes in monarch abundance in response to strong wind events, we deployed remote monitoring equipment near butterfly clusters at overwintering sites. Field observations utilized 15-meter telescoping fiberglass poles (Max-Gain Systems, Inc., Marietta, GA) anchored at three points using ground anchors with guy lines securing both the top and base to create stable, freestanding structures.

Poles were positioned 4-17 meters from cluster locations. This range, determined through field testing, balanced image resolution requirements for our grid-based counting method against disturbance minimization. Closer positioning compromised field of view, while greater distances degraded butterfly visibility below classification thresholds. Pole placement considered ground stability for the 15-meter structures, infras-

tructure clearance requirements, and clear viewing angles. When deploying near active clusters, we approached from directions that minimized disturbance; no butterfly dispersal was observed during equipment deployment.

We monitored monarch abundance using modified trail cameras (GardePro E7 and E8, Shenzhen, China) configured for near-infrared imaging to enhance contrast between clustering butterflies and surrounding vegetation. Trail cameras were selected for their durability for extended field deployment, native time-lapse functionality, and modification potential. Near-infrared wavelength selection followed previous literature demonstrating effectiveness for butterfly population estimation (Hristov, Nikolaidis, Hubel, & Allen, 2019).

Hardware modifications exploited the camera's internal filter-switching mechanism by engaging nighttime mode to access the clear glass filter position, then disconnecting power to prevent reversion to the infrared cut filter. Near-infrared pass filters (>850 nm) were mounted externally to restrict incoming light to NIR wavelengths. This configuration produced images where clustering butterflies appeared as dark masses against bright eucalyptus foliage reflectance in the near-infrared spectrum. Field validation confirmed sufficient contrast for visual distinction of monarch clusters from background vegetation, supporting our human-labeler analytical approach.

Cameras were mounted atop poles using lightweight tie-down straps and positioned horizontally toward butterfly clusters at roosting height. The wireless live view feature enabled real-time preview and precise camera aiming during deployment. Cameras operated in time-lapse mode with motion detection disabled.

Sampling interval selection balanced temporal resolution, battery life, and data processing feasibility through empirical optimization and rigorous statistical validation. Initial deployments used 10-minute intervals to capture significant changes in butterfly

abundance, which preliminary observations indicated occurred on hourly rather than minute scales, while maintaining approximately 6-week continuous operation. Post-deployment statistical analysis using mixed-effects models and information-theoretic approaches systematically compared multiple sampling intervals across deployments. We conducted sequential subsample analyses starting with full temporal resolution and progressively testing reduced frequencies. Information-theoretic model comparison using Akaike Information Criterion (AIC) demonstrated that 30-minute intervals provided optimal balance, losing less than 5% of information compared to full temporal resolution (measured by root mean square error) while reducing image classification workload by 67%. Variance comparison analysis and visual assessment of fitted trend lines confirmed that this interval preserved essential time-series patterns including diurnal activity cycles, weather-response dynamics, and multi-day population trends. Battery life constraints and field deployment logistics further supported this interval choice, enabling extended autonomous operation essential for capturing complete behavioral sequences during variable weather conditions.

To quantify the wind conditions hypothesized to influence butterfly behavior, wind monitoring equipment consisted of Rain Wise WindLog Wind Data Loggers (Rain Wise Inc., Trenton, Maine) installed at pole apices to measure wind at heights approximating butterfly roosting locations. These instruments recorded average wind speed and maximum wind gust at one-minute intervals, the highest frequency supported by the sensors. This recording interval enabled calculation of wind speed variance within each photographic sampling period, capturing gustiness lost with longer averaging periods.

To systematically organize our heterogeneous monitoring efforts, we defined discrete monitoring periods as deployment units. Each deployment represented a unique combination of monitoring location, camera configuration (including camera ID, mounting

height, and viewing angle), associated wind measurements, and temporal coverage period. Since equipment was frequently reused across locations and time periods, this deployment-based structure provided standardized sampling units that accounted for variation in environmental conditions and equipment configurations while treating each deployment as independent for statistical analyses. This approach produced time-series images from each deployment for estimating monarch cluster abundance through systematic grid-based counting methods, enabling analysis of abundance patterns in relation to wind speed and other environmental variables.

2.4 Image Analysis

2.5 Grid-based Counting Method

To quantify changes in monarch butterfly abundance from collected imagery, we developed a systematic grid-based counting protocol balancing accuracy with the practical constraints of analyzing tens of thousands of images. This approach addressed the challenge of estimating abundance in large aggregations where individual counts would be prohibitively time-consuming and emulated field researcher methods, including those used in the annual Thanksgiving Count (Xerces Society, 2018). We subdivided each image using a grid overlay system where human labelers assigned order-of-magnitude estimates per cell. Grid dimensions remained fixed throughout each deployment to ensure consistency. Custom software developed using the Electron framework in JavaScript facilitated this labeling effort.

Grid cell size varied by deployment based on camera-to-cluster distance. Cell dimensions were optimized to ensure most occupied cells contained butterflies in the 10–99 count range, balancing classification efficiency with spatial resolution. This stan-

dardization minimized cells alternating between widely different order-of-magnitude categories across the time series.

2.6 Counting Protocol

Human labelers estimated butterfly abundance within each grid cell using four order-of-magnitude categories: 0 (no butterflies), 1–9 (single digits), 10–99 (dozens), and 100–999 (hundreds). Labelers trained using a comprehensive online guide with example images and detailed classification criteria (https://kylenessen.github.io/monarch_trailcam_classifier/). The protocol prioritized efficiency while maintaining consistency across observers.

Because abundance estimates derived exclusively from two-dimensional photographic images, our classification protocol quantified only butterflies visible in the image plane without estimating three-dimensional cluster structure or depth. This approach intentionally excluded hidden individuals behind visible butterflies in overlapping aggregations, providing a conservative but consistent measure reflecting observable surface area rather than total volume. For cells containing partial butterflies at grid boundaries, labelers included these in counts unless double-counting would cause an adjacent cell to move to a higher category. When butterfly counts fluctuated between categories across the time series, we consistently applied the lower estimate to maintain conservative abundance estimates.

In addition to estimating monarch abundance, labelers recorded whether cells received direct sunlight. Direct sunlight classification presented challenges because oversaturated conditions eliminated the contrast enabling butterfly detection in shaded areas. Labelers classified cells as receiving direct sunlight when branches or butterflies exhibited additional illumination clearly from direct rather than indirect light, even

when individual butterflies became difficult to distinguish due to pixel oversaturation. This classification required careful attention to subtle shape recognition and contextual awareness about butterfly locations established from previous images in the time series. This measurement was recorded only for occupied cells and stored separately.

Labelers received ongoing feedback throughout the classification process. All classifications underwent review for common errors including mislabeled cells, incorrect category assignments, and inconsistent counting criteria application. Direct communication of corrections to labelers ensured consistent protocol application.

2.7 Abundance Calculation

We calculated an abundance index for each frame by summing the products of cell counts and their assigned category values across all grid cells, employing conservative estimates using minimum values within each order-of-magnitude category:

$$\text{Abundance index} = \sum_i \rho_i \times C_i \tag{2.1}$$

where ρ_i represents the number of cells in category i, and C_i represents the conservative estimate for that category. We used minimum category values ($C_1 = 1$ for category 1–9, $C_2 = 10$ for category 10–99, and $C_3 = 100$ for category 100–999) rather than midpoint or maximum values to ensure temporal analyses reflected genuine population shifts rather than estimation uncertainty.

2.8 Temperature Data Extraction

Temperature represents a critical environmental variable influencing monarch activity patterns and potentially confounding wind effects. Ambient temperature data were extracted from trail camera images using optical character recognition (OCR). Each camera displayed temperature readings on the image overlay, but these values were not accessible through EXIF metadata, necessitating visual extraction methods. We developed an automated Python script utilizing OCR technology to extract temperature values from approximately 56,000 images across all deployments. The extraction process employed multiple preprocessing strategies and pattern matching algorithms to accommodate variations in image quality and display characteristics.

Following initial automated extraction, we manually reviewed and corrected edge cases where OCR failed or produced anomalous values. All temperature data underwent systematic quality control through visualization of deployment-specific time series, enabling identification and correction of erroneous values. This process ensured complete temperature coverage for all analyzed images, providing the ambient temperature covariate required for our statistical models.

2.9 Statistical Analysis

2.10 Data Preparation

Statistical analysis employed a lag-based framework to capture the temporal dynamics of butterfly responses to environmental changes, comparing butterfly counts between consecutive 30-minute intervals. Observation pairs were constructed by matching counts at time t with counts at time $t - 30$ minutes, applying a ± 5 minute tolerance

window to accommodate minor temporal variations in image capture. The response variable (change in butterfly abundance between time points) underwent cube root transformation to achieve approximate normality while preserving directional information: $y = \text{sign}(\Delta) \times |\Delta|^{1/3}$, where Δ represents the difference in butterfly counts. While exploratory data analysis revealed generally well-behaved distributions, we observed bimodality in the raw butterfly abundance data driven primarily by a single anomalous event at deployment SC8. At this deployment, a large butterfly aggregation abruptly declined to near zero without corresponding changes in the measured environmental variables (wind speed, temperature, or solar exposure). This singular event was unlike any other observation in the dataset. We retained this deployment in the final analysis for two reasons: first, to maximize sample size and avoid arbitrary data exclusion, and second, sensitivity analysis showed that the cube root transformation of abundance differences adequately addressed the distributional concerns, with model selection and parameter estimates remaining consistent whether SC8 was included or excluded. The transformation approach made the anomaly's inclusion or exclusion immaterial to the final results. Observation pairs where both time points recorded zero butterflies were excluded as uninformative, reducing the dataset from approximately 2,500 potential pairs to 1,894 analyzable observations across 115 unique deployment-day combinations.

2.11 Variable Selection

Predictor variables were selected to test specific hypotheses while avoiding multicollinearity. Maximum wind gust speed during each 30-minute interval served as the primary wind metric, with alternative wind measurements (average sustained speed, modal gust, gust standard deviation) excluded due to high correlation ($r > 0.75$). Environmental predictors included average temperature between observation pairs,

number of butterflies in direct sunlight at the previous time point, and minutes elapsed since the first observation of each day to capture diurnal patterns. Total butterfly count at the previous time point was included as a control variable, enabling distinction between proportional and absolute changes in abundance. When included, this variable tests effects on proportional change; when excluded, models test effects on absolute change.

2.12 Model Framework

Analysis employed generalized additive mixed models (GAMMs) implemented through the mgcv package in R. Model selection followed an information-theoretic approach, comparing 52 candidate models using Akaike Information Criterion (AIC). The candidate set comprised two fundamental frameworks: models including the lag abundance term (24 models) and models excluding it (24 models), with each framework containing null models, single predictor models, additive combinations, two- and three-way interactions, and models incorporating smooth terms for non-linear relationships. Random effects structure accounted for variation at three hierarchical levels: deployment location, observer, and deployment-day. Temporal autocorrelation within days was addressed using a first-order autoregressive (AR1) correlation structure grouped by deployment-day. All models were fitted using restricted maximum likelihood (REML) estimation.

To test specifically for threshold effects at the proposed 2 m/s disruptive wind speed, we conducted a threshold wind disruption analysis using an alternative wind metric. We repeated the entire model selection process, replacing maximum wind gust speed with a threshold-based predictor: the count of minutes within each 30-minute observation period where wind gusts equaled or exceeded 2 m/s. This variable ranged from

0 to 30 minutes and was tested using the same 52 model structures, allowing direct comparison of continuous versus threshold-based wind effects.

2.13 Model Validation

Model assumptions were verified through standard residual diagnostics including examination of residual distributions, fitted versus residual plots, and quantile-quantile plots. Convergence was confirmed for all candidate models in both the primary and threshold wind disruption analyses. Model performance and predictor significance were evaluated through AIC comparison, with models differing by less than 2 AIC units considered equivalent.

2.14 Statistical Power Analysis

To evaluate whether our study had adequate statistical power to detect wind effects if present, we conducted a simulation-based power analysis. This approach assessed our ability to detect various effect sizes given our sample size of 1,894 paired observations. We simulated 200 datasets from the best-fitting model (which excluded wind effects) and artificially introduced wind effects of known magnitude ranging from 0.05 to 0.20 standard deviations of the response variable. For each effect size, we refitted models including wind terms to determine the proportion of simulations where the artificial effect was detected as statistically significant ($\alpha = 0.05$). This simulation approach accounts for the complexity of our GAMM framework and hierarchical data structure, providing robust estimates of statistical power for detecting wind effects across a range of biologically plausible magnitudes.

2.15 Dynamic Window Analysis

To examine whether day-to-day changes in roost size depend on cumulative weather exposure aligned with butterfly roosting biology, we conducted a complementary analysis using dynamic temporal windows. This approach tested wind effects at a daily scale, capturing overnight and full-day weather exposure that the 30-minute lag analysis could not assess.

We constructed two window definitions to test the robustness of our findings. The sunset window spanned from the previous day's maximum butterfly count to the current day's last observation, approximating functional sunset when roosting decisions finalize. This biologically-aligned window varied in duration (mean = 29.6 hours) to capture the complete exposure period from peak aggregation through the subsequent roosting decision point. The 24-hour window provided a standardized comparison, extending exactly 24 hours from the previous day's maximum count.

Daily aggregates were computed for each deployment-day combination, including maximum butterfly count, 95th percentile count, and mean of the top three counts. We retained only days with 15-25 daytime photographs to ensure adequate temporal coverage, then constructed consecutive day pairs separated by exactly one day. Pairs where both days recorded zero butterflies were excluded as uninformative. The response variable, defined as the change in maximum daily count between consecutive days, underwent signed square root transformation to achieve approximate normality while preserving directional information.

Weather metrics were calculated within each dynamic window. Temperature variables included minimum, maximum, and mean values, plus cumulative metrics such as degree-hours above 15°C. Wind measurements comprised average sustained speed,

maximum gust, cumulative gust exposure, and time above the proposed 2 m/s threshold. Direct sun exposure was quantified as the cumulative count of butterflies observed in direct sunlight across all frames within the window, integrating both exposure duration and instantaneous abundance. We required 95% data completeness across temperature, wind, and daylight observations, calculated as the geometric mean of coverage ratios.

Variable selection for the dynamic window analysis began with 19 candidate predictors spanning baseline abundance metrics, temperature summaries, wind exposure measures, and cumulative sun exposure. We conducted correlation analysis to identify multicollinearity within predictor families, particularly among the highly intercorrelated wind metrics (all pairwise correlations $r > 0.75$) and temperature variables. Based on this analysis, we selected predictors that minimized redundancy while maintaining interpretability and adequate degrees of freedom relative to sample size.

For wind exposure, we selected maximum wind gust as the primary metric because it captured the variance of all wind variables in a single interpretable measure, showed high correlation with sustained speed, gust summation, and threshold exceedance metrics, and maintained consistency with the 30-minute analysis. We excluded wind mode gust despite its biological relevance because it contained only approximately five unique values across the dataset, causing model convergence issues. Temperature representation focused on non-overlapping summaries that captured both the exposure range (minimum and maximum) and the thermal state at the previous day's peak abundance. We excluded highly correlated metrics such as mean temperature and degree-hours above 15°C to reduce multicollinearity. The cumulative direct sun exposure variable was retained as a biologically relevant measure of thermal conditions that integrated both exposure duration and instantaneous abundance. For the

sunset window analysis, we included lag duration (hours) as a control variable to account for varying window lengths.

Model selection followed the same information-theoretic approach as the 30-minute analysis. We evaluated 78 candidate models per window type using generalized additive mixed models with deployment random intercepts and AR(1) temporal correlation structures. The candidate set included null models, single predictors, additive combinations, and models with smooth interaction terms. To address potential overfitting given the reduced sample size (n = 94-96 pairs), we applied conservative thresholds for the ratio of effective degrees of freedom to sample size and conducted leave-one-deployment-out cross-validation on top-performing models. The final predictor set comprised: temperature minimum and maximum, maximum wind gust, cumulative direct sun exposure, and baseline abundance controls.

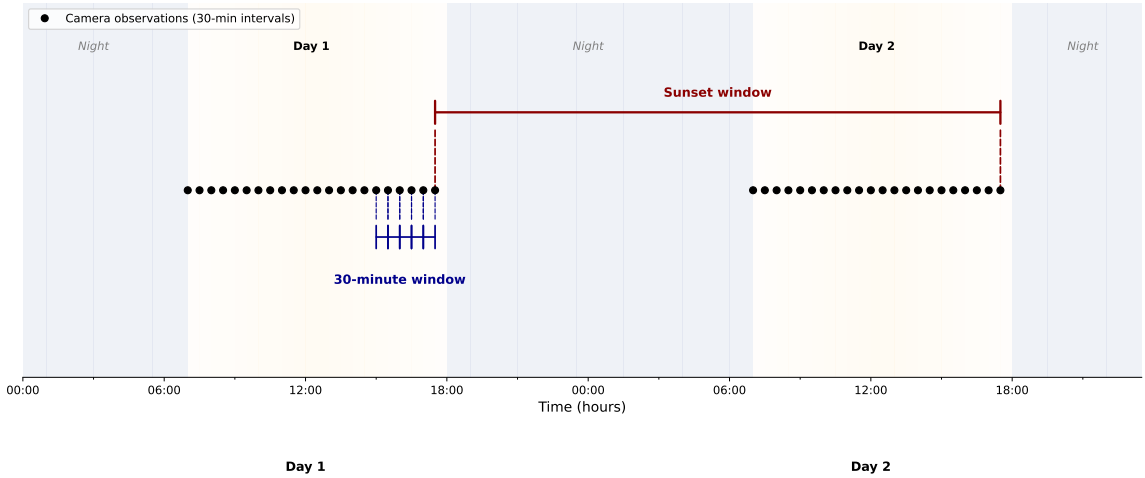

Figure 2.1: Temporal analysis windows for monarch butterfly monitoring. *The figure illustrates two complementary approaches: (1) 30-minute lag analysis comparing consecutive observation intervals to capture immediate responses to environmental changes, and (2) sunset window analysis spanning from the previous day's maximum butterfly count to the current day's final observation (mean duration ∼29.6 hours). Camera observations occur at 30-minute intervals during daylight hours only. Background shading indicates day-night cycles with transitions at sunrise and sunset.*

Chapter 3

RESULTS

3.1 Descriptive Statistics

Environmental conditions varied substantially across the 78-day monitoring period at Spring Canyon and UDMH during the 2023-2024 overwintering season. The dataset comprised 1,894 observations collected at 30-minute intervals during daylight hours (07:00–17:00) from November 17, 2023, to February 4, 2024, totaling 947 observation hours across 115 unique deployment-day combinations.

Wind speeds ranged from complete calm to moderately strong conditions, with maximum gusts reaching 12.4 m/s (mean = 2.2 ± 1.4 m/s, median = 2.2 m/s). The interquartile range of 1.3–3.0 m/s indicated that most observations occurred under relatively mild wind conditions. Temperatures showed considerable variation throughout the monitoring period, ranging from 3.0 to 30.0°C (mean = 14.6 ± 3.8°C, median = 14.0°C), with an interquartile range of 12.5–17.0°C typical of California coastal winter conditions. Direct solar exposure occurred in 31.7% of observations (n = 601), with butterflies actively basking when present in sunlight. When direct sunlight was available, an average of 17.0 individual butterflies occupied sunlit positions (range: 1–295), though most observations recorded no butterflies in direct sun, with the distribution heavily skewed toward low or zero values.

Monarch abundance exhibited high variability across sites and time periods. Butterfly counts ranged from 0 to 770 individuals per observation, with a mean of 81.4 ± 100.0 butterflies and a median of 37 butterflies. The wide interquartile range (9–119 butterflies) reflected substantial variation in cluster sizes. Zero-count observations,

representing either the beginning of cluster formation or cluster dissolution, comprised 2.3% of the dataset (n = 43).

Cluster sizes varied markedly among the 10 deployment locations. Site SC10 recorded the largest aggregation with 770 monarchs, while mean abundances ranged from 0 at SC9 to 325.8 at UDMH2. Eight deployments observed maximum cluster sizes exceeding 100 butterflies, with mean maximum cluster size across sites reaching 315.6 individuals. This variation in cluster sizes across deployments reflects the heterogeneous distribution of monarchs across overwintering microhabitats within the study sites.

The comprehensive temporal coverage, with observations at 30-minute intervals capturing 16.5 observations per deployment-day on average, provided fine-scale resolution of monarch behavioral responses to changing environmental conditions. Peak observation activity occurred at 16:00 hours (196 observations), corresponding with afternoon warming periods when monarchs typically exhibit increased movement.

3.2 Linear Regression Between Wind and Cluster Dynamics

Linear regression analyses examined whether wind speed alone could explain changes in monarch cluster size, revealing no meaningful relationship between maximum wind speed and cluster size changes at either temporal scale (Figure 3.1 and 3.2).

At 30-minute intervals, linear regression confirmed no statistically significant relationship between maximum wind speed and butterfly abundance change ($\beta = 1.19$ butterflies per m/s, SE = 0.66, p = 0.073, n = 1,894). The correlation was negligible (r = 0.041, $R^2 = 0.002$), with wind speed explaining only 0.17% of the variance in cluster size changes. Data points scattered uniformly across all wind speeds from calm

conditions to 12.4 m/s. The proposed 2 m/s behavioral threshold showed no apparent demarcation in butterfly responses, with similar variance in cluster size changes both above and below this threshold.

Day-to-day analyses similarly revealed no statistically significant relationship between maximum wind exposure and cluster size changes ($\beta = 5.34$ butterflies per m/s, SE = 4.63, p = 0.252, n = 101). The correlation remained weak (r = 0.115, $R^2 = 0.013$), with wind speed explaining only 1.3% of the variance in abundance changes between consecutive days. All observation periods in this analysis experienced maximum wind speeds exceeding the proposed 2 m/s behavioral threshold. Despite consistent exposure to winds above the threshold, no clear pattern emerged linking wind intensity to subsequent roost abandonment or growth.

These null linear regression relationships indicated that wind speed alone cannot predict monarch clustering behavior, necessitating examination of more complex environmental interactions and conditional relationships that may modulate wind effects.

3.3 Wind Disruption Analysis

To examine how monarchs respond to immediate environmental conditions, we analyzed 1,894 paired observations collected at 30-minute intervals throughout the overwintering season. This responsive change analysis tested whether short-term fluctuations in cluster size could be explained by concurrent weather variables, particularly wind exposure.

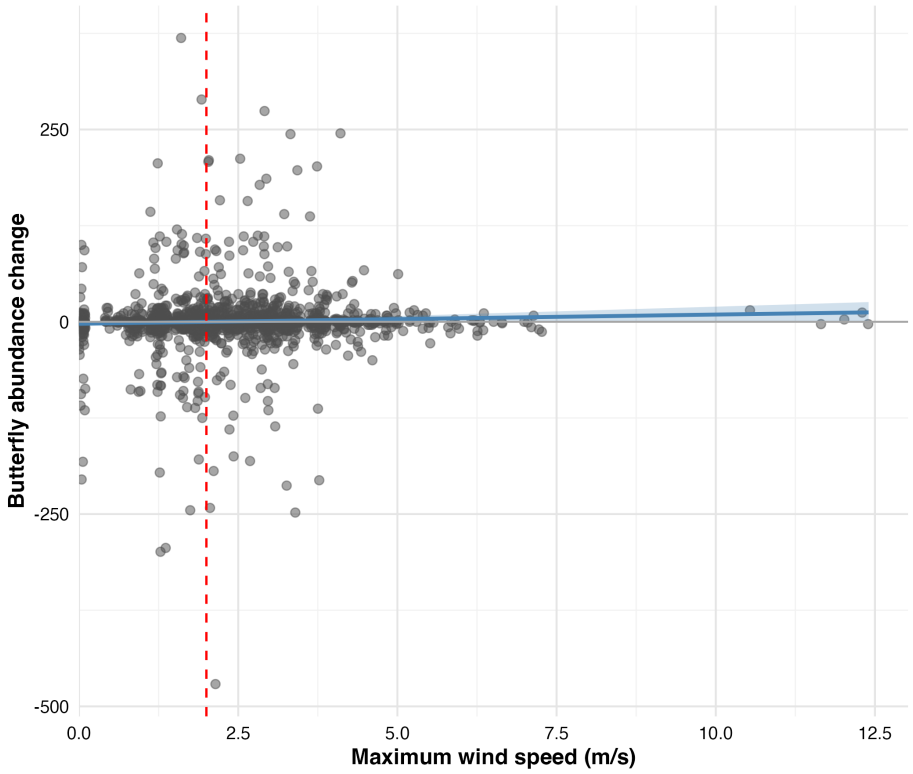

Figure 3.1: Wind speed vs. abundance change (30-minute). *Linear regression of maximum wind speed and butterfly abundance change at 30-minute intervals. Each point represents a paired observation (n = 1,894). Linear regression showed no significant relationship ($\beta = 1.19$, $SE = 0.66$, $p = 0.073$, $r = 0.041$, $R^2 = 0.002$). The red dashed line indicates the proposed 2 m/s behavioral threshold. The blue regression line is shown for reference despite non-significance.*

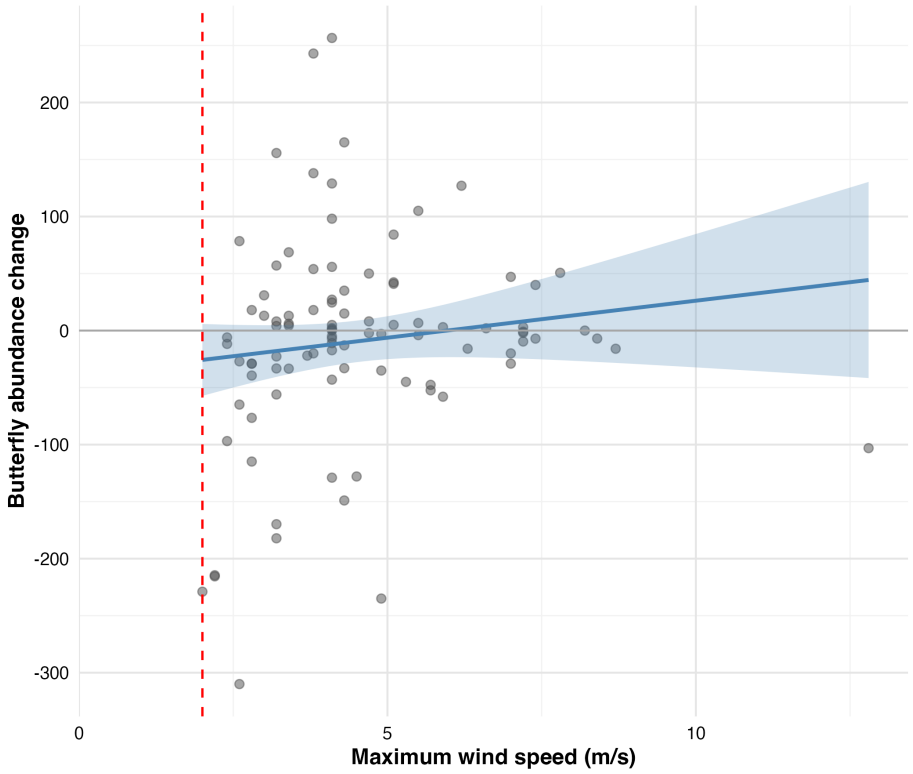

Figure 3.2: Wind speed vs. cluster size changes (day-to-day). *Linear regression of maximum wind speed and day-to-day cluster size changes from maximum count to next sunset. Each point represents consecutive day pairs at the same deployment ($n = 101$). Linear regression showed no significant relationship ($\beta = 5.34$, $SE = 4.63$, $p = 0.252$, $r = 0.115$, $R^2 = 0.013$). The red dashed line indicates the 2 m/s threshold. All observations experienced winds exceeding this threshold. The blue regression line is shown for reference despite non-significance.*

Table 3.1: Top 5 models ranked by AIC (30-minute analysis).

Model	Terms	AIC	ΔAIC	Weight
M50	Previous butterfly count, Temperature, Time since sunrise, Interaction (tensor): Maximum wind speed, Butterflies in direct sun	8074.03	0.00	0.86
M23	Previous butterfly count, Temperature, Butterflies in direct sun, Time since sunrise	8077.86	3.83	0.13
M22	Previous butterfly count, Temperature (linear), Butterflies in direct sun, Time since sunrise	8082.90	8.87	0.01
M24	Previous butterfly count, Maximum wind speed, Temperature, Butterflies in direct sun, Time since sunrise	8084.05	10.02	0.01
M52	Temperature, Time since sunrise, Interaction (tensor): Maximum wind speed, Butterflies in direct sun	8092.72	18.69	0.00

3.4 Model Selection: 30-Minute Analysis

In the 30-minute wind disruption analysis, we evaluated 52 candidate models using generalized additive mixed models (GAMMs) to identify the environmental predictors of monarch abundance changes. Model selection via Akaike Information Criterion (AIC) identified M50 as the decisively best-fit model, capturing 85.8% of the total model weight (Table 3.1). The next best model (M23) showed substantially weaker support with ΔAIC = 3.8 and only 12.6% model weight. Model M50 incorporated smoothed terms for previous butterfly count, temperature, and time of day (minutes since sunrise), along with a tensor interaction between maximum wind speed and butterflies in direct sun.

3.5 Analysis of Best Fit Model

The best-fit model from the 30-minute wind disruption analysis (M50) predicted change in butterfly abundance as a function of: (1) the previous 30-minute observation's butterfly count, (2) average temperature, (3) time of day, and (4) an interaction between maximum wind gust speed and the number of butterflies in direct sunlight.

Statistical analysis of the responsive change model revealed significant effects for three of the four predictors (Table 3.2). The previous butterfly count ($F = 12.50$, $p < 0.001$), time of day ($F = 9.85$, $p < 0.001$), and the wind-sunlight interaction ($F = 4.67$, $p < 0.001$) all showed strong statistical significance. Temperature effects approached but did not reach conventional significance thresholds ($F = 3.19$, $p = 0.057$). The model explained 6.4% of the variance in butterfly abundance changes (adjusted $R^2 = 0.064$, $n = 1894$).

Table 3.2: Summary of best-fit model (M50).

Smooth Term	**edf**	**Ref.df**	**F**	**p-value**
Previous butterfly count	2.41	2.41	12.50	< 0.001***
Average temperature	3.68	3.68	3.19	0.057
Time since sunrise	4.87	4.87	9.85	< 0.001***
Wind gust × Sunlight exposure	7.35	7.35	4.67	< 0.001***
Model performance: Adj. $R^2 = 0.064$, Scale est. $= 4.03$, $n = 1894$				

Partial effects for the smooth terms, which represent the isolated influence of each predictor while holding other variables constant, are shown in Figure 3.3. The previous butterfly count showed a significant non-linear negative relationship ($p < 0.001$) consistent with proportionally greater departures from larger aggregations. Time of day captured a significant diurnal pattern ($p < 0.001$) with morning departures and afternoon returns. Temperature showed a marginally non-significant trend ($p = 0.057$) suggesting possible effects near the 12.7–16°C flight threshold range.

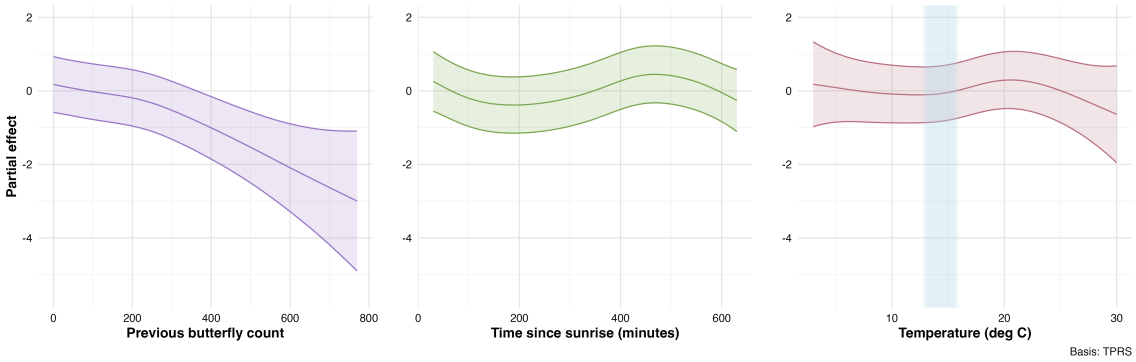

Figure 3.3: Partial effects of environmental predictors (M50). *Partial effects of environmental predictors on monarch butterfly abundance changes from the best-fit GAMM model (M50) in the 30-minute wind disruption analysis. Partial effects show how each environmental factor influences butterfly abundance while holding all other variables constant at their average values, isolating each predictor's individual contribution to the response. Shaded regions represent 95% confidence intervals.*

In the 30-minute wind disruption analysis, the tensor interaction between wind speed and butterflies in direct sun ($p < 0.001$) revealed a complex conditional relationship where wind effects depended on solar exposure conditions (Figure 3.4). When butterflies in direct sun were held at zero (all butterflies in indirect light), cluster size changes showed no consistent trend across the observed wind speed range (0–12 m/s). Conversely, when wind was held constant, low numbers of butterflies in direct sun were associated with decreasing cluster sizes across the time window, while higher counts led to increasing cluster sizes across the time window. At low butterfly counts in direct sun, the wind effect showed distinct patterns: clusters decreased in size at very calm winds <1 m/s, showed no change from 1–3 m/s, and tended to increase from 4–8 m/s. At moderate wind speeds (1–3 m/s) and high butterfly counts >100, cluster sizes tended to decrease. However, as wind speeds exceeded 3 m/s at these same butterfly counts, the pattern reversed, with cluster sizes increasing. The red dashed line at 2 m/s indicates the behavioral threshold identified in previous analyses. Gray regions mask areas too distant from observed data points for reliable interpretation, and caution is warranted when interpreting the strongest partial effects at

the edges of the data distribution, where observations are sparse and interpolation artifacts may occur. Notably, the overwhelming majority of observations occurred at very low butterfly counts in direct sun, emphasizing that most clustering behavior happens when few butterflies are exposed to direct sunlight.

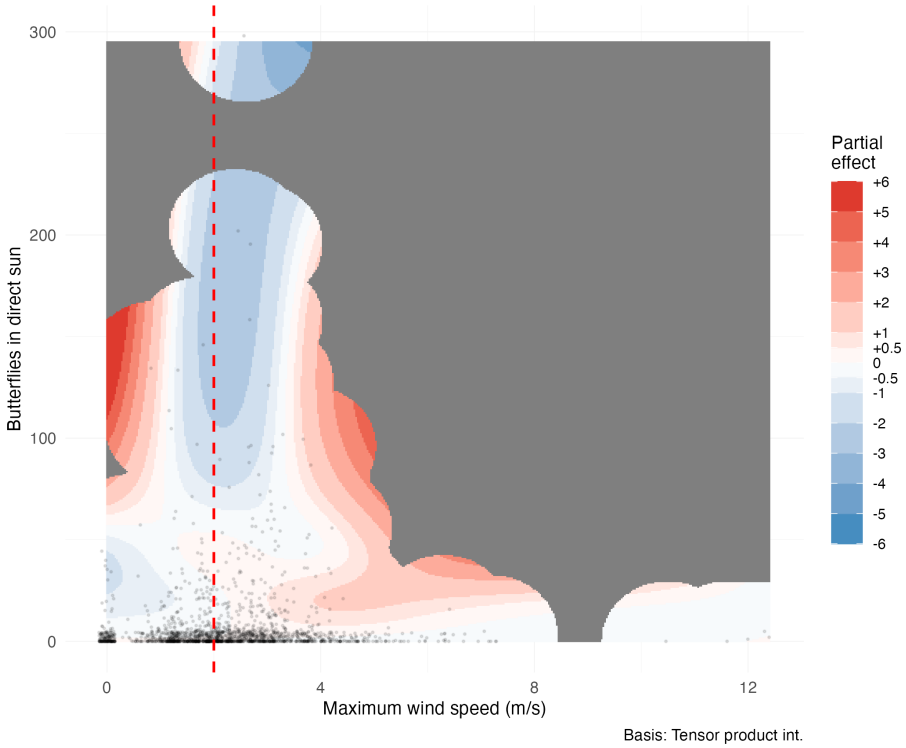

Figure 3.4: Wind × sunlight interaction (30-minute analysis). *Tensor smooth interaction between maximum wind speed (m/s) and butterflies in direct sun on cluster size changes in the 30-minute wind disruption analysis. Color gradient indicates partial effect magnitude (red = positive, blue = negative). Black points show observed data distribution. Red dashed line marks the 2 m/s behavioral threshold. Gray regions indicate areas beyond reliable interpolation range.*

3.6 Model Diagnostics

Model diagnostic plots confirmed the adequacy of the GAMM specification (Figure 3.5). Residual versus fitted value plots showed no systematic patterns or heteroscedasticity, indicating appropriate model structure. The quantile-quantile plot

revealed approximately normal residual distribution with minor deviations in the tails.

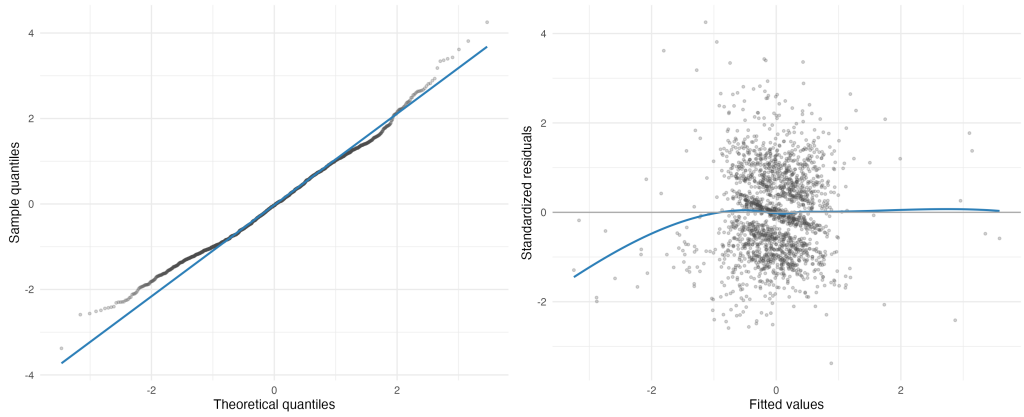

Figure 3.5: Diagnostic plots (M50). *Diagnostic plots for the best-fit GAMM model (M50). Left panel shows quantile-quantile plot comparing model residuals to theoretical normal distribution. Right panel displays residuals versus fitted values to assess homoscedasticity and model adequacy.*

Basis dimension checks confirmed adequate smoothing parameter selection for all model terms (Table 3.3). All smooth functions showed k-index values near 1.0, indicating sufficient basis dimensions to capture the underlying functional forms. None of the smooth terms showed evidence of undersmoothing (all p-values > 0.05), with the possible exception of time within day which showed marginal evidence (k-index $= 0.96$, p $= 0.065$). These diagnostics confirm that the chosen basis dimensions adequately represent the complexity of the smooth relationships without overfitting.

Table 3.3: Basis dimension adequacy checks (M50).

Smooth Term	k'	edf	k-index	p-value
s(total butterflies t_{lag})	9.00	2.41	1.00	0.735
s(temperature avg)	9.00	3.67	1.02	0.895
s(time within day t)	9.00	4.87	0.96	0.065
ti(max gust, butterflies direct sun t_{lag})	16.00	7.35	0.99	0.490

Temporal autocorrelation analysis revealed minimal residual correlation structure after accounting for the AR(1) correlation within deployment days (Figure 3.6). The

autocorrelation function showed rapid decay with all lags beyond lag 1 falling within the significance bounds, confirming that the model adequately captured temporal dependencies in the data. This indicates that our mixed-effects structure with autoregressive errors appropriately addressed the repeated measures nature of the time-series observations.

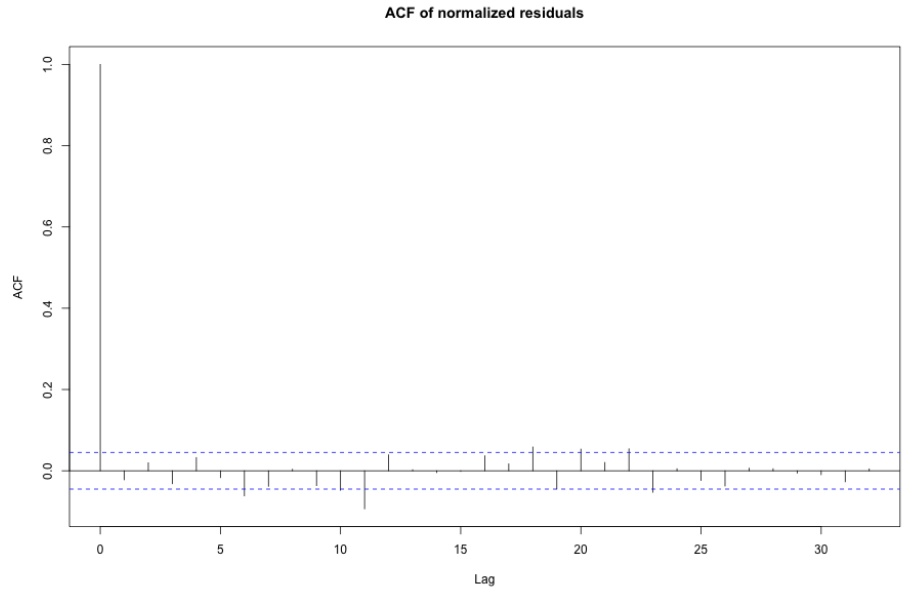

Figure 3.6: Autocorrelation function (M50). *Autocorrelation function of model residuals showing minimal temporal correlation after accounting for AR(1) structure within deployment days. Blue dashed lines indicate 95% confidence bounds for white noise.*

3.7 Threshold Wind Disruption Analysis

Within the 30-minute wind disruption analysis framework, we conducted this threshold analysis to determine whether wind is best characterized as a continuous variable or a binary disruption threshold, regardless of whether it operates independently or conditionally on other factors. To test the hypothesis that wind acts as a binary disruption threshold rather than a continuous variable, we repeated the entire 30-minute interval analysis using minutes above 2 m/s as the wind predictor. This threshold-

Table 3.4: Top 5 models ranked by AIC (30-minute threshold analysis).

Model	Terms	AIC	ΔAIC	Weight
T50	Previous butterfly count, Temperature, Time since sunrise, Interaction (tensor): Minutes above 2 m/s, Butterflies in direct sun	8077.23	0.00	0.55
T23	Previous butterfly count, Temperature, Butterflies in direct sun, Time since sunrise	8077.86	0.63	0.40
T22	Previous butterfly count, Temperature (linear), Butterflies in direct sun, Time since sunrise	8082.90	5.67	0.03
T24	Previous butterfly count, Minutes above 2 m/s, Temperature, Butterflies in direct sun, Time since sunrise	8085.41	8.18	0.01
T47	Temperature, Butterflies in direct sun, Time since sunrise	8097.30	20.07	0.00

based approach directly tests our second hypothesis that wind becomes disruptive above the 2 m/s threshold, which, if it represents a meaningful biological boundary, should predict declining monarch abundance at roosts experiencing sustained winds exceeding this threshold. The best threshold model (T50) maintained the same structure as our primary analysis but showed notably weaker performance (Table 3.4).

While T50 achieved the lowest AIC among threshold models, it failed to decisively outperform simpler alternatives, capturing only 55.4% of model weight compared to 40.4% for the model without any wind term (T23). The negligible difference in AIC (ΔAIC = 0.63) between these models indicates substantial certainty that the threshold wind variable does not substantially improve predictions. Despite this weaker overall performance (adjusted $R^2 = 0.061$ compared to 0.064 in the primary analysis), the interaction term between minutes above threshold and butterflies in direct sun achieved statistical significance ($p = 0.0001$), and notably, T50 was the only model among the top five candidates to include any wind parameters. This suggests that while the threshold approach may not optimally characterize wind effects, the interaction with solar exposure warrants examination.

The interaction partial effects plot from the 30-minute threshold analysis reveals complex conditional relationships between wind exposure duration and solar conditions (Figure 3.7). When butterflies in direct sun are held at zero (all butterflies in indirect light), cluster size changes show no apparent trend across the entire range of wind exposure duration, from no time above threshold to the full 30-minute observation period. This suggests that wind effects on shaded butterflies are minimal regardless of exposure duration.

As butterfly counts in direct sun increase, distinct patterns emerge. At moderate counts (25-50 butterflies), cluster sizes tend to decrease when wind exposure extends from 15 to 25 minutes above threshold. However, at the extremes of sustained wind exposure (greater than 25 minutes), cluster sizes tend to increase. When wind exposure is minimal (0-5 minutes above threshold), increasing butterfly counts in sun show no effect on cluster size changes. The strongest effects appear at intermediate wind exposure durations (15-25 minutes) combined with moderate solar exposure levels.

The same caveats apply regarding sparse data at the extremes and the limits of interpolation, particularly given that most observations occurred at low butterfly counts in direct sun.

3.8 Statistical Power to Detect Wind Effects

Post-hoc power analysis confirmed our study had adequate statistical power to detect biologically meaningful wind effects (Table 3.5). With 1,894 paired observations, we achieved 87.5% power to detect moderate effect sizes (0.15 standard deviations) and 98.5% power to detect larger effects (0.20 standard deviations). Power for small effects (0.10 standard deviations) was 56%, while very small effects (0.05 standard

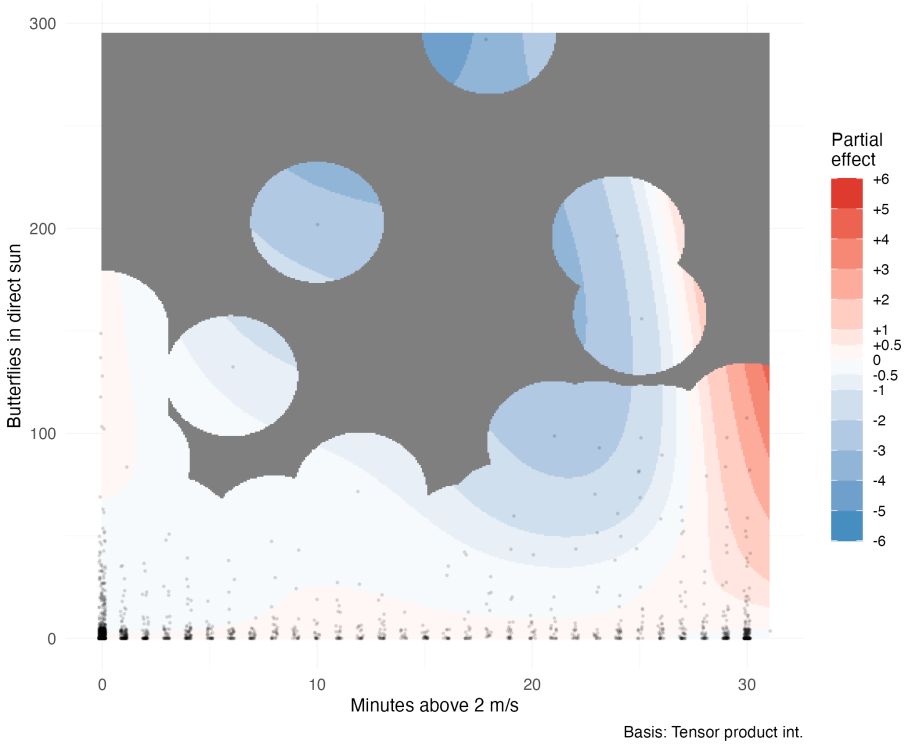

Figure 3.7: Wind threshold × sunlight interaction. *Tensor smooth interaction between minutes above 2 m/s wind threshold and butterflies in direct sun on cluster size changes. Color gradient indicates partial effect magnitude (red = positive, blue = negative). Black points show observed data distribution. Gray regions indicate areas beyond reliable interpolation range.*

deviations) yielded only 16.5% power. These results indicate that our study has sufficient statistical power for effect sizes of biological relevance.

Table 3.5: Statistical power to detect wind effects.

Effect Size (SD units)	Power (Proportion)	Power (%)
0.05	0.05	0.165	16.5%
0.1	0.10	0.560	56%
0.15	0.15	0.875	87.5%
0.2	0.20	0.985	98.5%

3.9 Site Fidelity Analysis

The preceding wind disruption analysis examined how monarchs respond to immediate environmental conditions, testing whether strong wind events trigger the rapid cluster departures predicted by the behavioral disruption hypothesis. While our 30-minute analysis revealed no simple relationship between wind speed and cluster changes, it assumed butterflies could respond instantaneously to unfavorable conditions. This assumption may not hold when adverse conditions occur during periods when temperatures fall below the flight threshold, constraining monarchs' ability to relocate until environmental conditions permit flight. Furthermore, monarchs may make clustering decisions on longer temporal horizons than our 30-minute observation intervals capture. To address these limitations, we conducted a complementary analysis examining day-to-day roost dynamics by tracking clusters from one day's maximum count through the following day's sunset, when darkness precludes further aggregation changes. This approach tests whether cumulative weather exposure over extended periods influences site fidelity decisions, with substantial decreases in cluster size indicating reduced site suitability and potential roost abandonment, while stable or increasing counts suggest the site remains suitable despite weather exposure.

To implement this day-to-day analysis, we examined 96 consecutive-day pairs from the same deployment dataset using biologically-aligned temporal windows. The primary analysis employed a sunset window spanning from the previous day's maximum count to the current day's last observation (mean duration = 29.6 hours), capturing the full period from peak aggregation through the subsequent roosting decision. A secondary analysis using fixed 24-hour windows (n = 94 pairs) provided a sensitivity test of our findings.

Daily maximum cluster sizes ranged from 0 to 770 butterflies (mean = 134.7 ± 138.1), with day-to-day changes in maximum count ranging from losses of 376 butterflies to gains of 464 butterflies (mean change = -10.5 ± 111.6). Within the sunset windows, maximum wind gusts ranged from 2.0 to 12.8 m/s (mean = 4.5 ± 1.8 m/s), with all observation windows exceeding the proposed 2 m/s threshold. Cumulative direct sun exposure varied from 0 to 1,122 butterfly-observations in sunlight per window (mean = 139.8 ± 206.9), reflecting diverse thermal exposure conditions across monitoring days.

3.10 Model Selection: Site Fidelity Analysis

We evaluated 78 candidate models using generalized additive mixed models (GAMMs) to identify environmental predictors of day-to-day changes in maximum cluster size. The model space included null, single-predictor, interaction-only, additive, main effects with interactions, and complex formulations, all incorporating deployment random intercepts and AR(1) temporal correlation. Model selection via corrected Akaike Information Criterion (AICc) identified the best-fit model (M32) as the decisively best-fit model, capturing 84.7% of the total model weight (Table 3.6). The next best model (M52) showed substantially weaker support with ΔAICc = 5.6 and only 5.2%

Table 3.6: Top 5 models ranked by AICc (sunset analysis).

Model	Terms	AICc	ΔAICc	Weight
M32	Interaction (tensor): Maximum wind gust, Cumulative butterflies in direct sun	648.85	0.00	0.85
M52	Maximum wind gust, Cumulative butterflies in direct sun, Interaction (tensor): Maximum wind gust, Cumulative butterflies in direct sun	654.45	5.60	0.05
M20	Interaction (tensor): Minimum temperature, Cumulative butterflies in direct sun	656.77	7.92	0.02
M46	Maximum temperature, Cumulative butterflies in direct sun, Interaction (tensor): Maximum temperature, Cumulative butterflies in direct sun	657.70	8.85	0.01
M30	Interaction (tensor): Temperature at previous maximum count, Cumulative butterflies in direct sun	657.90	9.06	0.01

model weight. Model M32 incorporated a tensor smooth interaction between maximum wind gust and cumulative direct sun exposure, along with baseline controls for previous day's maximum count and window duration.

3.11 Analysis of Best Fit Model

The best-fit model (M32) predicted square-root transformed change in butterfly abundance as a function of: (1) the previous day's maximum butterfly count, (2) window duration in hours, and (3) a tensor smooth interaction between maximum wind gust speed and cumulative butterflies in direct sunlight.

Statistical analysis revealed significant effects for the previous day's maximum count ($F = 24.88$, $p < 0.001$) and the wind-sunlight interaction ($F = 4.10$, $p < 0.001$), while window duration showed no significant effect ($F = 1.14$, $p = 0.289$) (Table 3.7). The day-to-day site fidelity model explained 39.7% of the variance in cluster size changes (adjusted $R^2 = 0.397$, $n = 96$), representing substantially greater explanatory power

than the 30-minute wind disruption analysis (adjusted $R^2 = 0.064$). This six-fold improvement in explanatory power suggests that cumulative weather exposure over day-long periods is more strongly associated with roosting decisions than immediate short-term conditions, supporting the hypothesis that monarchs integrate environmental conditions over extended time periods when making site fidelity decisions.

Table 3.7: Summary of best-fit model (M32).

Smooth Term	**edf**	**Ref.df**	**F**	**p-value**
Previous day maximum count	1.00	1.00	24.88	$< 0.001^{***}$
Window duration	1.00	1.00	1.14	0.289
Wind gust × Sunlight exposure	6.68	6.68	4.10	$< 0.001^{***}$
Model performance: Adj. $R^2 = 0.397$, Scale est. = 41.06, n = 96				

The previous day's maximum count showed a significant negative linear relationship (coefficient = -0.030, SE = 0.006), indicating that larger clusters experienced proportionally greater losses between days. This pattern aligns with the 30-minute wind disruption analysis findings. Window duration showed no significant relationship with cluster size changes. Partial effects for these linear predictors are shown in Figure 3.8.

In the day-to-day site fidelity analysis, the tensor smooth interaction between maximum wind gust and cumulative direct sun exposure ($p < 0.001$) revealed complex conditional relationships between sustained weather exposure and cumulative butterflies in direct light (Figure 3.9). All observations during the study period experienced wind speeds exceeding 2 m/s. Under low wind speeds around 2 m/s with minimal butterfly counts in direct sun, clusters increased the following day, though this pattern reversed sharply as butterfly counts increased, resulting in decreased cluster sizes. When butterfly counts approached zero, cluster sizes showed minimal change to slight decreases across most wind speeds, with the exception of extreme wind values where sparse data limits interpretation. At intermediate to high values of both wind speed and butterfly sun exposure, cluster sizes increased the next day. These patterns sug-

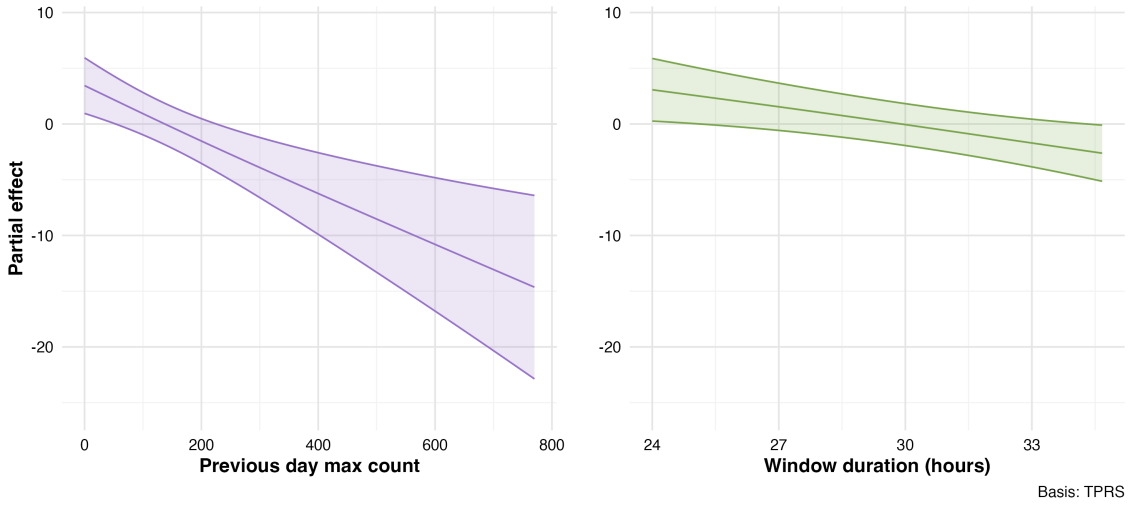

Figure 3.8: Partial effects of control variables (M32). *Partial effects of control variables on day-to-day monarch butterfly cluster size changes from the best-fit GAMM model (M32). Partial effects isolate how each variable influences cluster size changes while holding other factors constant at their average values. Left panel shows the strong negative effect of previous day maximum count. Right panel shows window duration had no significant effect on cluster size changes. Shaded regions represent 95% confidence intervals.*

gest monarchs redistribute within the grove, moving from deployments experiencing unfavorable conditions (blue regions showing cluster decreases) to deployments with more favorable conditions (red regions showing cluster increases), though movements may also occur between monitored and unmonitored areas of the grove or involve butterflies entering or leaving the site. Interpretation requires caution at interpolation boundaries and regions with single observations.

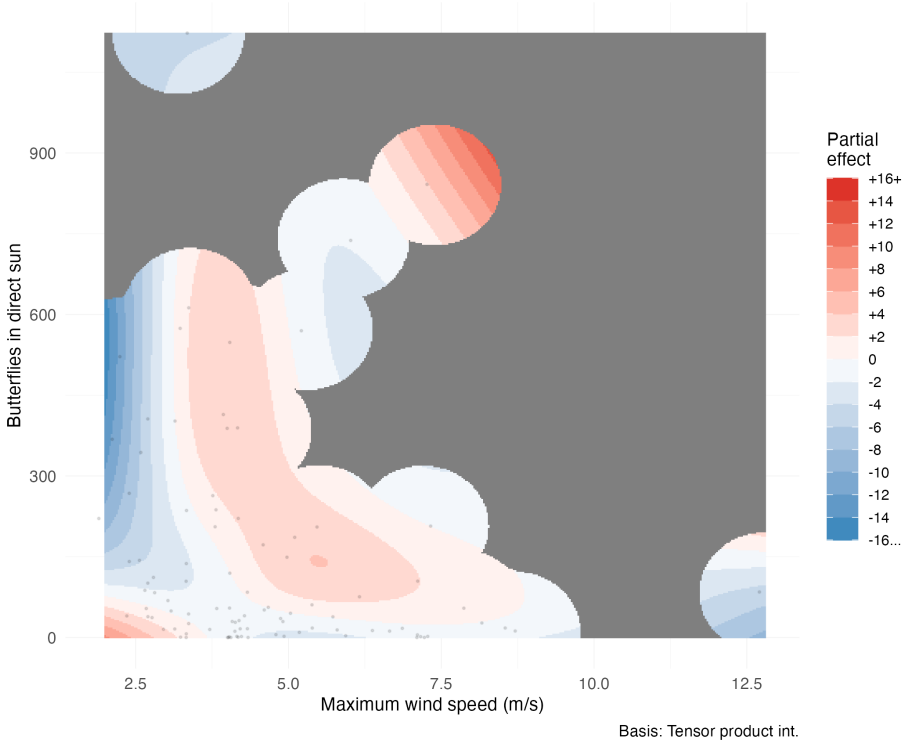

Figure 3.9: Wind × sunlight interaction (day-to-day analysis). *Tensor smooth interaction between maximum wind gust (m/s) and cumulative butterflies in direct sun on day-to-day cluster size changes. Color gradient indicates partial effect magnitude on square-root transformed scale (red = positive, blue = negative). Black points show observed data distribution. Gray regions indicate areas beyond reliable interpolation range.*

3.12 Model Diagnostics

Model diagnostic plots confirmed the adequacy of the GAMM specification (Figure 3.10). Residual versus fitted value plots showed no systematic patterns or heteroscedasticity, indicating appropriate model structure. The quantile-quantile plot revealed approximately normal residual distribution with minor deviations in the tails.

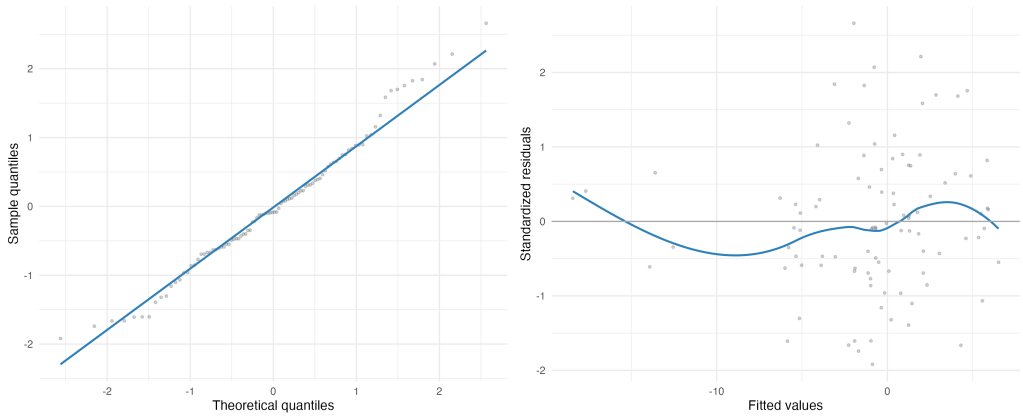

Figure 3.10: Diagnostic plots (M32). *Diagnostic plots for the best-fit GAMM model (M32). Left panel shows quantile-quantile plot comparing model residuals to theoretical normal distribution. Right panel displays residuals versus fitted values to assess homoscedasticity and model adequacy.*

Basis dimension checks confirmed adequate smoothing parameter selection for the tensor smooth interaction term. The wind-sunlight interaction showed a k-index value of 1.06 ($p = 0.72$), indicating sufficient basis dimensions to capture the underlying functional form without evidence of undersmoothing. This confirms that the chosen basis dimensions adequately represent the complexity of the smooth relationship without overfitting.

Temporal autocorrelation analysis revealed minimal residual correlation structure after accounting for the AR(1) correlation within deployment days (Figure 3.11). The

autocorrelation function showed rapid decay with all lags beyond lag 1 falling within the significance bounds, confirming that the model adequately captured temporal dependencies in the data.

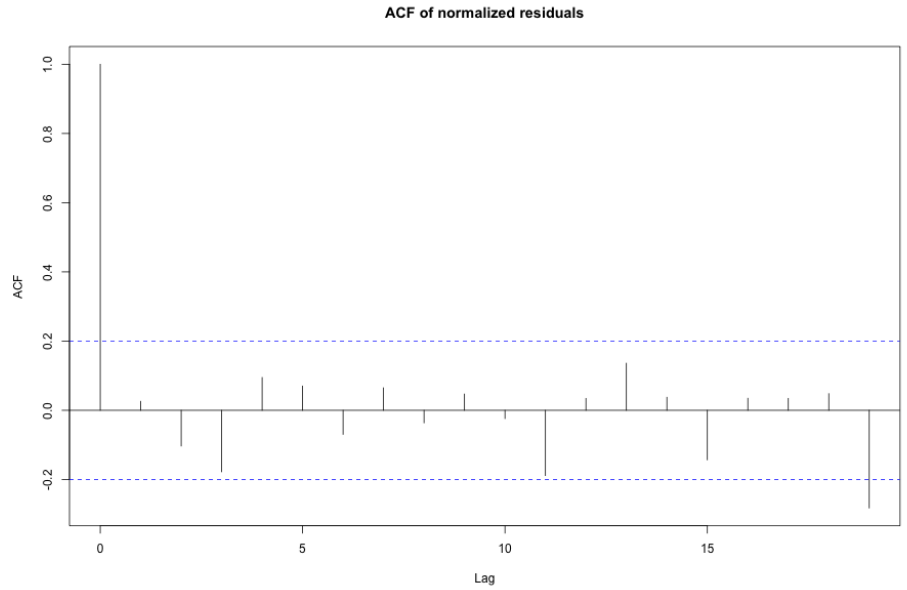

Figure 3.11: Autocorrelation function (M32). *Autocorrelation function of model residuals showing minimal temporal correlation after accounting for AR(1) structure within deployment days. Blue dashed lines indicate 95% confidence bounds for white noise.*

3.13 Robustness Analysis: 24-Hour Butterfly Change

To assess the robustness of our day-to-day site fidelity findings, we conducted an analysis examining butterfly cluster changes over 24-hour periods rather than sunset-specific intervals. This analysis evaluated the same 76 candidate models using identical GAMM specifications with deployment random intercepts and AR(1) temporal correlation. Notably, model selection converged on the same structural form as the primary day-to-day site fidelity analysis. Model M31, incorporating a tensor smooth interaction between maximum wind gust and cumulative direct sun exposure, emerged as the decisively best-fit model with 50.7% of the total model weight (Table 3.8).

Alternative models showed substantially weaker support, with the next best model achieving only 8.4% weight and ΔAICc = 3.6.

Table 3.8: Top models from 24-hour robustness analysis.

Model	Description	AICc	ΔAICc	Weight	adj. R^2
M31	Wind × sun exposure (smooth)	636.3	0.0	0.507	0.235
M23	Temperature × wind (smooth)	639.9	3.6	0.084	–
M29	Temperature × sun exposure (smooth)	640.8	4.4	0.056	–
M19	Min. temp. × sun exposure (smooth)	641.1	4.8	0.047	–
M51	Wind + sun + wind×sun (smooth)	641.7	5.4	0.034	–

The 24-hour robustness analysis revealed qualitatively similar interaction patterns to the day-to-day site fidelity analysis, though with attenuated effect magnitudes reflecting the longer temporal window (Figure 3.12). Under low wind conditions (approximately 2 m/s) with minimal butterflies in direct sun, clusters increased over the subsequent 24 hours. This effect reversed sharply as butterfly counts in direct sun increased under low winds, resulting in rapid cluster size decreases. When no butterflies occupied direct sun positions, cluster sizes remained relatively stable across wind speed values. Intermediate values for both wind speed and sun exposure produced cluster size increases. The convergent model selection and consistent interaction patterns across temporal scales strengthen confidence in the identified environmental relationships, while interpretation requires similar caution near data boundaries and regions with sparse observations.

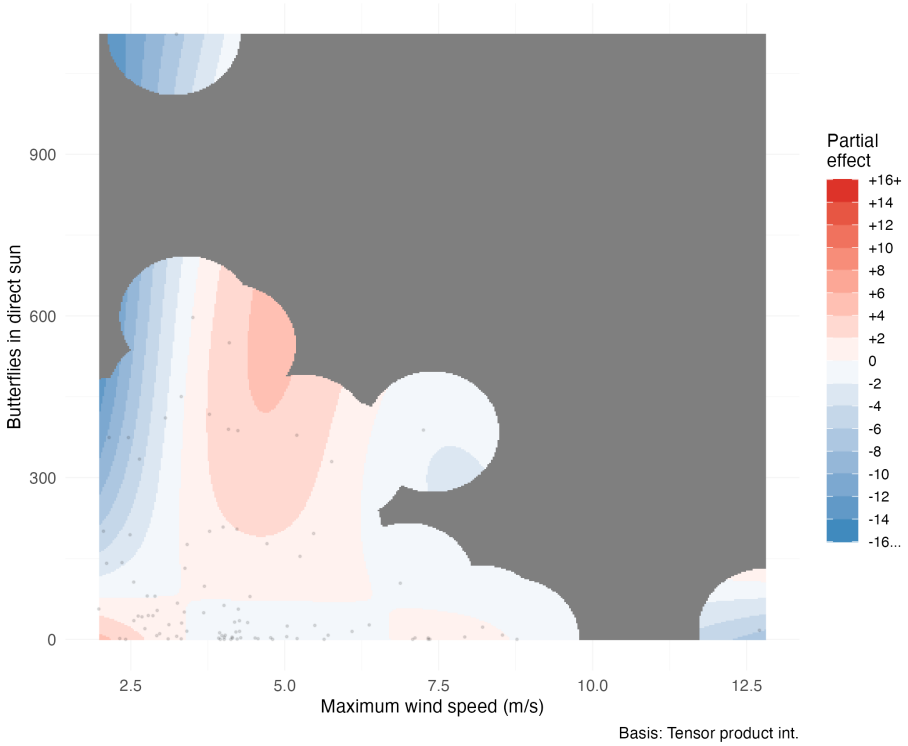

Figure 3.12: Wind × sunlight interaction (24-hour robustness). *Tensor smooth interaction between maximum wind gust (m/s) and cumulative butterflies in direct sun on 24-hour cluster size changes. Color gradient indicates partial effect magnitude on square-root transformed scale (red = positive, blue = negative). Black points show observed data distribution. Gray regions indicate areas beyond reliable interpolation range. The interaction pattern mirrors that observed in the sunset-specific analysis, supporting the robustness of identified environmental relationships.*

Chapter 4

DISCUSSION

Our study provides the first direct empirical test of the long-standing hypothesis that wind disrupts overwintering monarch butterfly clusters. For over three decades, conservation practice has operated under the assumption that wind speeds exceeding 2 m/s force butterflies to abandon their roosts, either by physically dislodging them or triggering behavioral departures (K. L. H. Leong, 2016). Our findings challenge this fundamental assumption. Though there does appear to be a 'wind effect,' it is not at 2 m/s nor the only effect, and instead, our results suggest a more complex relationship between monarchs and their overwintering environment.

4.1 Evidence Against Wind Disruption

The evidence against the wind disruption hypothesis emerges from multiple, independent lines of analysis. Most strikingly, every single observation period in our sunset analysis experienced maximum wind speeds exceeding the proposed 2 m/s threshold (range: 2.0–12.8 m/s), yet monarch clusters persisted throughout the 78-day study period. If the hypothesis were correct, we should have observed either mass departures when temperatures permitted flight or butterflies physically dislodged and littering the ground when too cold to fly, as described in the literature (K. L. H. Leong, 1999). We observed neither.

When we examined the simple relationship between wind speed and cluster size changes, we found essentially no correlation at either temporal scale (30-minute $R^2 = 0.002$, n = 1,894; sunset $R^2 = 0.013$, n = 96). These analyses tested the most basic

prediction of the hypothesis that increasing wind speed should produce decreasing cluster sizes. The absence of this relationship across wind speeds ranging from calm conditions to six times the proposed threshold suggests that wind alone does not drive clustering decisions.

While wind alone showed no disruptive effect, our models revealed that monarchs respond to environmental conditions through complex interactions, particularly between wind and solar exposure. The wind-sunlight interaction achieved statistical significance in both temporal analyses (30-minute: $F = 4.67$, $p < 0.001$; sunset: $F = 4.10$, $p < 0.001$), emerging as the only environmental interaction significant across both timescales. Critically, this interaction demonstrates that wind effects depend entirely on light conditions: when butterflies remained in shade, wind speed had no effect on cluster dynamics across the full range of observed speeds (0 to 12.4 m/s), while the relationship became complex and conditional only when butterflies occupied sunlit positions. This pattern indicates that wind does not act as an independent disruptive force but rather modulates butterfly responses to solar exposure, fundamentally challenging the notion of wind as a primary limiting factor.

Statistical power was not a limitation. Our analysis achieved 87.5% power to detect moderate effects and 98.5% power for large effects. The wind disruption hypothesis predicts substantial, observable impacts, not subtle statistical signals. Our failure to detect these effects, despite adequate power and validated methodology that successfully identified other environmental signals, provides strong evidence against the hypothesis rather than merely absence of evidence.

4.2 Thermoregulation as an Alternative Explanation

The nature of these wind-light interactions requires careful consideration. During our study, butterflies rarely experienced direct sunlight, with most observations recording few or no butterflies in sun. This natural behavioral pattern meant that our models extrapolated interaction effects into data-sparse regions, particularly at high sun exposure values where fewer than 3% of observations occurred. The patterns we describe therefore reflect a combination of robust findings in data-rich conditions (primarily shaded butterflies) and model predictions in less-observed states (that reflected a different dynamic).

The clearest finding emerges from our most common condition: when butterflies remained in shade, wind speed had no effect on cluster dynamics across the entire observed range (0 to 12.4 m/s). This pattern was consistent across both our 30-minute and sunset analyses. Only isolated observations at the highest wind speeds, >10 m/s, showed any deviation, where single data points in otherwise unsampled regions produced unreliable model predictions, yet even these outliers directly contradicted the wind disruption hypothesis. The interaction patterns at higher sun exposure, while statistically significant, derive largely from model interpolation beyond our data-rich conditions, as fewer than 3% of observations occurred at high sun exposure values. Notably, our sunset analysis revealed that butterflies tended to depart from areas experiencing high light with low wind, yet showed increased abundance in areas with similar light levels when accompanied by higher wind speeds. The 30-minute and sunset analyses showed contrasting patterns under these wind-sun combinations: at moderate wind speeds with high butterfly sun exposure, the 30-minute analysis predicted cluster growth while the sunset analysis predicted cluster decline, potentially reflecting distinct behavioral responses operating at immediate versus overnight tem-

poral scales. These results suggest that light exposure may influence butterfly movement decisions, with wind conditions potentially modifying the response rather than acting as an independent disruptive force.

The pattern of butterflies responding differently to sunlit locations depending on wind conditions, combined with the complete absence of wind effects in shade, suggests that thermal considerations may underlie these behaviors. These patterns suggest thermoregulation as a plausible mechanism. Monarchs appear to both seek and avoid sunny locations depending on their thermal state. Masters, Malcolm, and Brower (1988) demonstrated that cold monarchs actively seek sun. The seeking allows warming from below flight threshold (12.7°C) to well above it within one minute through solar basking at ambient temperatures as low as 9°C. This represents an energetic advantage over the alternative warming mechanism, as Kammer (1970) showed that shivering requires 25 to 31 times more energy than resting. However, Masters, Malcolm, and Brower (1988) also found that monarchs avoid sun when thoracic temperatures approach 30°C. Monarchs depart sunny clusters to avoid overheating and excessive lipid depletion.

The model-predicted increases in cluster size at intermediate wind and sun levels could reflect a thermoregulatory balance where wind moderates the heating effects of solar exposure. Masters, Malcolm, and Brower (1988) observed that monarchs dissipate heat while gliding through airflow across their bodies. Similarly, environmental wind could provide passive convective cooling, as described by Riddell and Porter (2025), who found that wind-driven convective cooling interacts strongly with solar radiation effects in terrestrial organisms. This cooling mechanism might allow butterflies to remain in sunny locations longer than they otherwise would, with wind offsetting some of the solar heat gain that would typically trigger departure. In contrast, shaded butterflies experience no solar heat gain, making wind-driven cooling unnecessary and

potentially explaining the absence of wind effects in shade. However, the contrasting patterns between our immediate (30-minute) and sunset temporal scales suggest that multiple behavioral mechanisms may operate simultaneously, while other explanations could also produce these statistical patterns. Rather than attempting to definitively resolve these mechanisms with limited data from specific conditions, our findings point toward the importance of light exposure as a driver of butterfly behavior, warranting focused investigation of how canopy structure and resulting light regimes influence cluster dynamics.

Additional observations align with thermal management. Time since sunrise revealed strong diurnal patterns (30-minute $F = 9.85$, $p < 0.001$), with butterflies departing clusters in late morning and early afternoon, then reforming aggregations later in the day. This pattern persisted after controlling for temperature and sunlight, potentially reflecting endogenous circadian rhythms, though it also aligns with predictable daily thermal cycles. The midday dispersal may reflect routine activities such as patrolling flights or nectaring. Monarchs have been observed gliding during these dispersal periods, which could facilitate thermoregulatory cooling while accomplishing other essential behaviors. Our study could not follow individual butterflies once they departed cluster locations, so these activities remain speculative. Similar temporal patterns have been consistently documented at California overwintering sites (Chaplin & Wells, 1982; Tuskes & Brower, 1978), and the Xerces Society's standardized monitoring protocols explicitly restrict counting to specific time windows to account for these diurnal movements (Xerces Society, 2017).

Our models explained 6.4% of variance in 30-minute cluster changes and 39.7% of variance in sunset roost fidelity. The environmental factors that did explain variance were predominantly thermal in nature: the wind-light interaction, direct sunlight exposure, and diurnal patterns of dispersal and aggregation. While substantial variation

remains unexplained, the environmental signals we detected suggest thermal factors may play a more important role than wind avoidance in organizing clustering behavior. Without direct body temperature measurements under varying environmental conditions, thermoregulation remains one plausible interpretation among potentially others, and further research is needed to confirm the underlying mechanisms.

4.3 Limitations and Context

Several factors shape the interpretation of our findings. First, our data come from a single overwintering season (2023–2024) when monarch populations were relatively typical (Xerces Society, 2025a). The following season saw near-complete absence of monarchs at our study sites, coinciding with the second-lowest overwintering population on record (Xerces Society, 2025b). This dramatic population crash prevented temporal replication but underscores the urgency of understanding overwintering ecology with the data we have.

Second, our study observed relatively small clusters where butterflies maintained direct contact with eucalyptus substrates. The wind disruption hypothesis was developed during an era of massive aggregations containing hundreds of thousands of individuals, where many butterflies attached only to other butterflies in multi-layered formations (L. P. Brower, Williams, Fink, et al., 2008; K. L. H. Leong, 1990). If substrate attachment provides greater wind resistance than butterfly-to-butterfly attachment, wind might affect these different clustering configurations differently. The hypothesis may have been accurate for the extreme densities of past decades but less relevant to today's smaller populations.

Finally, our models explained relatively little variance overall (30-minute 6.4%; sunset 39.7%), reflecting both the complexity of butterfly behavior and our focus on test-

ing specific hypotheses rather than comprehensively explaining movement patterns. However, the strong signals we did detect and our adequate statistical power give confidence in our main conclusion that wind alone does not disrupt monarch clusters as previously believed.

4.4 Implications for Conservation

Our findings suggest that wind protection, long considered a limiting environmental factor in overwintering monarch conservation, may constrain habitat suitability far less than previously believed. This realization carries important implications for how we understand, manage, and restore overwintering sites.

4.5 Expanded Habitat Availability and Population Limitations

The absence of wind disruption despite frequent threshold exceedances indicates that suitable habitat within existing groves may be more extensive than currently recognized. Areas previously dismissed due to wind exposure might support clusters if they provide appropriate thermal and light conditions. With western monarch populations at historically low levels, this raises an important question: are we observing limited suitable habitat, or limited butterflies to occupy potentially suitable space? At historical abundances, monarchs may have utilized far more locations within groves than currently expressed. The small clusters we documented may represent only a fraction of available habitat, with suitable but unoccupied areas going unrecognized simply because too few butterflies exist to reveal these possibilities.

4.6 Simplified Management Requirements

Previous management frameworks required protecting extensive buffer zones around clustering sites. For example, Althouse & Meade, Inc. and Creekside Science (2023) recommended maintaining trees up to six tree heights from clustering locations to ensure adequate wind protection. For mature eucalyptus reaching 40 meters, this translates to protecting all trees within approximately 240 meters, creating substantial complexity in coastal California where overwintering sites often involve diverse stakeholders and contentious land use decisions.

If wind protection plays a less critical role than assumed, these extensive buffer requirements may no longer be necessary. Trees distant from core groves, previously considered essential for wind breaks, may contribute far less than previously thought. This simplification focuses conservation efforts more precisely on immediate grove structure rather than attempting to control wind patterns across vast surrounding areas.

However, a precautionary approach remains warranted. Where buffer trees exist as healthy, mature specimens, maintaining them represents prudent hedging against incomplete understanding. This temporal asymmetry, where removing trees or modifying canopy structure is always possible while accelerating large tree growth is not, argues for maintaining existing trees wherever possible. Previous recommendations to plant trees, maintain them for longevity, and develop succession plans remain entirely valid, even if the mechanistic understanding of why these practices work requires updating.

4.7 Proactive Habitat Creation Through Canopy Management

If monarchs respond primarily to light and thermal patterns rather than strict wind thresholds, strategic canopy modification may create new overwintering habitat. The wind protection framework offered little beyond planting trees and waiting decades for maturation. Light-based management might enable shorter-timeframe interventions.

Real-world examples support this possibility. At Monarch Lane in Los Osos, strategic canopy opening resulted in monarchs appearing and persisting (K. L. H. Leong, 1999; Xerces Society, 2025a). At Andrew Molera State Park in Big Sur, clearing an overgrown grove increased butterfly counts from zero to over one thousand (E. Pelton, personal communication). Conversely, tree planting at Pacific Grove required approximately 15 years of canopy maturation before monarchs returned (S. Weiss, personal communication). These patterns suggest that appropriate canopy structure, including carefully designed openings creating dappled light, can attract butterflies far more quickly than waiting for tree growth alone.

Unidentified eucalyptus stands or overly dense groves might thus be converted to functional habitat through selective thinning. However, additional research is needed before implementing large-scale canopy modifications, particularly at established overwintering sites. Rather than passive waiting, managers might proactively create suitable conditions by strategically opening existing canopies at appropriate locations, representing a significant departure from previous approaches focused almost entirely on wind protection and tree growth.

4.8 Long-term Optimism Despite Current Uncertainty

While this study reduces certainty regarding some aspects of overwintering ecology, the long-term trajectory points toward management practices that may be simpler to implement, are grounded in empirical evidence, and potentially are outright effective instead of simply more effective. The strict 2 m/s threshold created an overly constraining understanding of habitat requirements, suggesting suitable sites were overly limited. Our results indicate monarchs may be more resilient to environmental variation than previously believed, potentially revealing more opportunities for habitat creation and maintenance.

The fundamental conservation tools remain unchanged: maintaining existing groves, planting and managing trees for longevity, and developing succession plans for aging forests. But we may now recognize more locations where habitat might be suitable and fewer absolute constraints on where sites can be maintained or created. As Saniee and Villablanca (2022) suggest, managing canopy structure to create appropriate light patterns and temperature gradients may prove more important than achieving specific wind speed thresholds. This perspective aligns with our finding that interactions between environmental factors, rather than single variables in isolation, shape clustering behavior.

Conservation efforts should continue protecting forest structure at overwintering sites while research clarifies the specific environmental factors, particularly light patterns and thermal regimes, that monarchs select for when choosing roost locations.

4.9 Future Research Directions

Our findings open several important avenues for future research. While the wind-light interaction we observed suggests complex relationships between environmental factors and clustering behavior, the strong effect of light exposure itself points toward canopy structure as a potentially primary driver of habitat selection. This conclusion finds support in Saniee and Villablanca (2022), who found that while temperature and humidity failed to support the microclimate hypothesis at aggregation locations, solar radiation was one of the few environmental factors that distinguished occupied sites from other grove locations. Similarly, Weiss, Rich, Murphy, et al. (1991) found that successful overwintering sites maintain consistent canopy openness around 20%, while unsuccessful sites show greater variability. Combined with our findings, this suggests that predictable light patterns created by canopy structure may provide a stable, reliable environmental cue that monarchs can consistently locate and respond to year after year. Unlike weather conditions that fluctuate unpredictably, the spatial pattern of light created by canopy architecture remains relatively constant across seasons, offering a dependable signal for site selection. Monarchs possess sophisticated visual systems that enable sun compass navigation during migration (Mouritsen & Frost, 2002; Nguyen, Beetz, Merlin, & el Jundi, 2021), capabilities that would allow them to detect and respond to consistent light patterns within groves. Future research should prioritize characterizing canopy structure and the resulting light regimes at both occupied and unoccupied sites to determine whether specific light patterns predict roost site selection and fidelity.

Beyond environmental factors, social dynamics may explain additional variation in our models. The strong effect of previous butterfly count on subsequent changes suggests that monarchs do not distribute randomly within groves but rather exhibit

overdispersed clustering patterns where the presence of butterflies attracts others. This positive feedback mechanism, where initial settlement increases the probability of others joining, could create self-reinforcing aggregation patterns independent of immediate environmental conditions (Berdahl, Torney, Ioannou, et al., 2013).

Finally, testing these patterns across the broader overwintering range would establish their generality. Sites with different tree species, latitudes, and especially population densities could reveal whether wind responses vary with clustering configuration or if our findings represent fundamental aspects of monarch overwintering behavior.

4.10 Conclusions

Our direct test of the wind disruption hypothesis found no evidence that wind speeds above 2 m/s force monarchs to abandon their clusters. Every observation in our sunset analysis exceeded this threshold, yet clusters persisted. Linear regression analyses showed no relationship between wind and cluster changes. Model selection consistently identified other factors as more important. These multiple lines of evidence converge on a clear conclusion. Wind alone does not disrupt overwintering monarch butterflies as has been assumed for over three decades.

Instead, our results suggest that thermal factors may play a more important role in clustering dynamics than previously recognized. Monarchs responded strongly to direct sunlight and diurnal patterns, both factors that could influence body temperature. The unexpected wind-light interaction, where moderate wind combined with sun exposure sometimes increased cluster sizes, suggests that environmental conditions interact in complex ways that simple threshold-based management approaches cannot capture.

These findings arrive at a critical moment for monarch conservation. With western populations at historic lows, every assumption about habitat requirements deserves scrutiny. While questions remain about the precise mechanisms, our findings demonstrate that current management guidelines based on wind speed thresholds are not supported by empirical evidence. Moving forward, conservation efforts should prioritize maintaining existing overwintering groves while additional research clarifies what environmental factors monarchs select for when choosing roost sites. As we face the challenge of preserving overwintering habitat for a declining population, evidence-based understanding of monarch ecology becomes not just scientifically important, but essential for preserving the remarkable phenomenon of monarch migration in western North America.

REFERENCES

Alonso-Mejia, A., & Arellano-Guillermo, A. (1992). Influence of Temperature, Surface Body Moisture and Height Aboveground on Survival of Monarch Butterflies Overwintering in Mexico. *Biotropica*, *24*(3), 415–419. https://doi.org/10.2307/2388612

Althouse & Meade, Inc. & Creekside Science. (2023, April). *Ellwood Mesa/Sperling Preserve Open Space Monarch Butterfly Overwintering Habitat Analysis and Recommendations For Restoration*. City of Goleta - Public Works Department. Goleta, CA.

Barker, J. F., & Herman, W. S. (1976). Effect of photoperiod and temperature on reproduction of the monarch butterfly, *Danaus plexippus*. *Journal of Insect Physiology*, *22*(12), 1565–1568. https://doi.org/10.1016/0022-1910(76)90046-9

Baudier, K. M., D'Amelio, C. L., Malhotra, R., O'Connor, M. P., & O'Donnell, S. (2018). Extreme Insolation: Climatic Variation Shapes the Evolution of Thermal Tolerance at Multiple Scales. *The American Naturalist*, *192*(3), 347–359. https://doi.org/10.1086/698656

Bell, W. J., & Kramer, E. (1979). Search and anemotactic orientation of cockroaches. *Journal of Insect Physiology*, *25*(8), 631–640. https://doi.org/10.1016/0022-1910(79)90112-4

Berdahl, A., Torney, C. J., Ioannou, C. C., Faria, J. J., & Couzin, I. D. (2013). Emergent Sensing of Complex Environments by Mobile Animal Groups. *Science*, *339*(6119), 574–576. https://doi.org/10.1126/science.1225883

Bidlingmayer, W. L., Day, J. F., & Evans, D. G. (1995). Effect of wind velocity on suction trap catches of some Florida mosquitoes. *Journal of the American Mosquito Control Association*, *11*(3), 295–301.

Blois-Heulin, C., Crowley, P. H., Arrington, M., & Johnson, D. M. (1990). Direct and indirect effects of predators on the dominant invertebrates of two freshwater littoral communities. *Oecologia*, *84*(3), 295–306. https://doi.org/10.1007/BF00329753

Bonte, D., & Lens, L. (2007). Heritability of spider ballooning motivation under different wind velocities. *Evolutionary Ecology Research*, *9*, 817–827.

Brower, L. (1995). Understanding and misunderstanding the migration of the monarch butterfly (Nymphalidae) in North America: 1857-1995. *Journal of The Lepidopterists Society*. Retrieved December 7, 2024, from https://www.semanticscholar.org/paper/Understanding-and-misunderstanding-the-migration-of-Brower/79380ddbf559e310fef9bb8919c03c63ccddecb7

Brower, L. P., Williams, E., Fink, L., Zubieta, R., & Ramírez, M. (2008). Monarch butterfly clusters provide microclimatic advantages during the overwintering season in Mexico. *Journal of the Lepidopterists' Society*, *62*, 177–188.

Calvert, W. H., Zuchowski, W., & Brower, L. P. (1983). The Effect of Rain, Snow and Freezing Temperatures on Overwintering Monarch Butterflies in Mexico. *Biotropica*, *15*(1), 42–47. https://doi.org/10.2307/2387997

Chaplin, S. B., & Wells, P. H. (1982). Energy reserves and metabolic expenditures of monarch butterflies overwintering in southern California. *Ecological Entomology*, *7*(3), 249–256. https://doi.org/10.1111/j.1365-2311.1982.tb00664.x

Chown, S. L., Sørensen, J. G., & Terblanche, J. S. (2011). Water loss in insects: An environmental change perspective. *Journal of Insect Physiology*, *57*(8), 1070–1084. https://doi.org/10.1016/j.jinsphys.2011.05.004

Cockrell, B. J., Malcolm, S. B., & Brower, L. P. (1993). Time, temperature, and latitudinal constraints on the annual recolonization of eastern North America by the monarch butterfly. *Biology and conservation of the monarch butterfly*, *38*, 233–251. Retrieved September 26, 2025, from https://hero.epa.gov/hero/index.cfm/reference/details/reference_id/52731

Crone, E. E., Pelton, E. M., Brown, L. M., Thomas, C. C., & Schultz, C. B. (2019). Why are monarch butterflies declining in the West? Understanding the importance of multiple correlated drivers. *Ecological Applications*, *29*(7). https://doi.org/10.1002/eap.1975

Everatt, M. J., Convey, P., Bale, J. S., Worland, M. R., & Hayward, S. A. L. (2015). Responses of invertebrates to temperature and water stress: A polar perspective. *Journal of Thermal Biology*, *54*, 118–132. https://doi.org/10.1016/j.jtherbio.2014.05.004

Fisher, A., Saniee, K., Van der Heide, C., Griffiths, J., Meade, D., & Villablanca, F. (2018). Climatic Niche Model for Overwintering Monarch Butterflies in a Topographically Complex Region of California. *Insects*, *9*(4), 167. https://doi.org/10.3390/insects9040167

Freedman, M. G., de Roode, J. C., Forister, M. L., Kronforst, M. R., Pierce, A. A., Schultz, C. B., Taylor, O. R., & Crone, E. E. (2021). Are eastern and western monarch butterflies distinct populations? A review of evidence for ecological, phenotypic, and genetic differentiation and implications for conservation. *Conservation Science and Practice*, *3*(7), e432. https://doi.org/10.1111/csp2.432

Goehring, L., & Oberhauser, K. S. (2002). Effects of photoperiod, temperature, and host plant age on induction of reproductive diapause and development time in Danaus plexippus. *Ecological Entomology*, *27*(6), 674–685. https://doi.org/10.1046/j.1365-2311.2002.00454.x

Hanrahan, S. A., & and Kirchner, W. H. (1997). The effect of wind on foraging activity of the tenebrionid beetle Lepidochora discoidalis in the sand dunes of the Namib Desert. *South African Journal of Zoology*, *32*(4), 136–139. https://doi.org/10.1080/02541858.1997.11448445

Herman, W. S., & Tatar, M. (2001). Juvenile hormone regulation of longevity in the migratory monarch butterfly. *Proceedings of the Royal Society B: Biological Sciences*, *268*(1485), 2509–2514. https://doi.org/10.1098/rspb.2001.1765

Hristov, N. I., Nikolaidis, D., Hubel, T. Y., & Allen, L. C. (2019). Estimating Overwintering Monarch Butterfly Populations Using Terrestrial LiDAR Scanning. *Frontiers in Ecology and Evolution*, *7*. Retrieved October 13, 2022, from https://www.frontiersin.org/articles/10.3389/fevo.2019.00266

Jepsen, S., Pelton, E., Black, S. H., Fallon, C., Voight, C., & Weiss, S. B. (2017). *Protecting California's Butterfly Groves: Management Guidelines for Monarch Butterfly Overwintering Habitat*. The Xerces Society for Invertebrate Conservation. Portland, OR. https://xerces.org/protecting-californias-butterfly-groves

Jepsen, S., Schweitzer, D. F., Young, B., Sears, N., Ormes, M., & Black, S. H. (2015, March). *Conservation Status and Ecology of the Monarch Butterfly in the United States* (15-016_01). Arlington, VA, Portland, OR. https://www.xerces.org

Jepsen, S. J., & Black, S. H. (2015). Understanding and Conserving the Western North American Monarch Population. In K. S. Oberhauser, K. R. Nail, & S. Altizer (Eds.), *Monarchs in a changing world: Biology and conservation of an iconic butterfly* (pp. 147–156). Cornell University Press.

Kammer, A. E. (1970). Thoracic temperature, shivering, and flight in the monarch butterfly, Danaus plexippus (L.) *Zeitschrift für vergleichende Physiologie*, *68*(3), 334–344. https://doi.org/10.1007/BF00298260

Lafferty, K. D., & Shaw, J. C. (2013). Comparing mechanisms of host manipulation across host and parasite taxa. *Journal of Experimental Biology*, *216*(1), 56–66. https://doi.org/10.1242/jeb.073668

Leonard, R. J., McArthur, C., & Hochuli, D. F. (2016). Exposure to wind alters insect herbivore behaviour in larvae of Uraba lugens (Lepidoptera: Nolidae). *Austral Entomology*, *55*(3), 242–246. https://doi.org/10.1111/aen.12175

Leong, K. L. H. (1999). Restoration of an overwintering grove in Los Osos, San Luis Obispo County, California. *1997 North American Conference on the Monarch Butterfly. Eds. J. Hoth, L. Merino, K. Oberhauser, I. Pisanty, S. Price, and T. Wilkinson*, 221–218.

Leong, K. L. H. (1990). Microenvironmental Factors Associated with the Winter Habitat of the Monarch Butterfly (Lepidoptera: Danaidae) in Central California. *Annals of the Entomological Society of America*, *83*(5), 906–910. https://doi.org/10.1093/aesa/83.5.906

Leong, K. L. H. (2016). Evaluation and Management of California Monarch Winter Sites.

Leong, K. L., Frey, D., Brenner, G., Baker, S., & Fox, D. (1991). Use of Multivariate Analyses to Characterize the Monarch Butterfly (Lepidoptera: Danaidae) Winter Habitat. *Annals of the Entomological Society of America*, *84*(3), 263–267. https://doi.org/10.1093/aesa/84.3.263

Marini, L., & Zalucki, M. P. (2017). Density-dependence in the declining population of the monarch butterfly. *Scientific Reports*, *7*. https://doi.org/10.1038/s41598-017-14510-w

Masters, A. R., Malcolm, S. B., & Brower, L. P. (1988). Monarch Butterfly (Danaus Plexippus) Thermoregulatory Behavior and Adaptations for Overwintering in Mexico. *Ecology*, *69*(2), 458–467. https://doi.org/10.2307/1940444

Miller-ter Kuile, A., Apigo, A., Bui, A., DiFiore, B., Forbes, E. S., Lee, M., Orr, D., Preston, D. L., Behm, R., Bogar, T., Childress, J., Dirzo, R., Klope, M., Lafferty, K. D., McLaughlin, J., Morse, M., Motta, C., Park, K., Plummer, K., ... Young, H. (2022). Predator–prey interactions of terrestrial invertebrates are determined by predator body size and species identity. *Ecology*, *103*(5), e3634. https://doi.org/10.1002/ecy.3634

Mouritsen, H., & Frost, B. J. (2002). Virtual migration in tethered flying monarch butterflies reveals their orientation mechanisms. *Proceedings of the National Academy of Sciences of the United States of America*, *99*(15), 10162–10166. https://doi.org/10.1073/pnas.152137299

Nathan, R., Sapir, N., Trakhtenbrot, A., Katul, G. G., Bohrer, G., Otte, M., Avissar, R., Soons, M. B., Horn, H. S., Wikelski, M., & Levin, S. A. (2005). Long-distance biological transport processes through the air: Can nature's complexity be unfolded in silico? *Diversity and Distributions*, *11*(2), 131–137. https://doi.org/10.1111/j.1366-9516.2005.00146.x

Nguyen, T. A. T., Beetz, M. J., Merlin, C., & el Jundi, B. (2021). Sun compass neurons are tuned to migratory orientation in monarch butterflies. *Proceedings of the Royal Society B: Biological Sciences*, *288*(1945), 20202988. https://doi.org/10.1098/rspb.2020.2988

Pelton, E. (2020, October). *Monarch Butterfly Overwintering Site Management Plan for Pismo State Beach: North Beach Campground Site*. The Xerces Society for Invertebrate Conservation. Pismo State Beach, California.

Pelton, E. M., Schultz, C. B., Jepsen, S. J., Black, S. H., & Crone, E. E. (2019). Western Monarch Population Plummets: Status, Probable Causes, and Recommended Conservation Actions. *Frontiers in Ecology and Evolution*, *7*. Retrieved January 11, 2023, from https://www.frontiersin.org/articles/10.3389/fevo.2019.00258

Reppert, S. M., & de Roode, J. C. (2018). Demystifying Monarch Butterfly Migration. *Current Biology*, *28*(17), R1009–R1022. https://doi.org/10.1016/j.cub.2018.02.067

Riddell, E. A., & Porter, C. K. (2025). The Wind Niche: The Thermal and Hydric Effects of Wind Speed on Terrestrial Organisms. *Integrative and Comparative Biology*, icaf025. https://doi.org/10.1093/icb/icaf025

Saniee, K., & Villablanca, F. (2022). Hierarchy and Scale Influence the Western Monarch Butterfly Overwintering Microclimate. *Frontiers in Conservation Science*, *3*. Retrieved May 16, 2023, from https://www.frontiersin.org/articles/10.3389/fcosc.2022.844299

Schultz, C. B., Brown, L. M., Pelton, E., & Crone, E. E. (2017). Citizen science monitoring demonstrates dramatic declines of monarch butterflies in western North America. *Biological Conservation*, *214*, 343–346. https://doi.org/10.1016/j.biocon.2017.08.019

Schweizer, M., Triebskorn, R., & Köhler, H.-R. (2019). Snails in the sun: Strategies of terrestrial gastropods to cope with hot and dry conditions. *Ecology and Evolution*, *9*(22), 12940–12960. https://doi.org/10.1002/ece3.5607

Solensky, M. J. (2004). Overview of monarch migration. In K. S. Oberhauser & M. J. Solensky (Eds.), *The monarch butterfly: Biology and conservation* (pp. 79–83). Cornell University Press.

The Monarch Press. (2019, June). *City Awarded $3.9 Million in Funding for the Monarch Butterfly Habitat Management Plan.* Retrieved February 9, 2024, from https://www.goletamonarchpress.com/2019/06/city-awarded-3-9-million-in-funding-for-the-monarch-butterfly-habitat-management-plan/

Tuskes, P. M., & Brower, L. P. (1978). Overwintering ecology of the monarch butterfly, Danaus plexippus L., in California. *Ecological Entomology*, *3*(2), 141–153. https://doi.org/10.1111/j.1365-2311.1978.tb00912.x

Urquhart, F. A., & Urquhart, N. R. (1978). Autumnal migration routes of the eastern population of the monarch butterfly (*Danaus p. plexippus* L.; Danaidae; Lepidoptera) in North America to the overwintering site in the Neovolcanic Plateau of Mexico. *Canadian Journal of Zoology*, *56*(8), 1759–1764.

U.S. Fish and Wildlife Service. (2024, December). *Monarch (Danaus plexippus) Species Status Assessment Report* (version 2.3). Washington, DC. https://www.fws.gov/media/monarch-butterfly-danaus-plexippus-species-status-assessment-report-version-23

Velilla, E., Muñoz, M., Quiroga, N., Symes, L., ter Hofstede, H. M., Page, R. A., Simon, R., Ellers, J., & Halfwerk, W. (2020). Gone with the wind: Is signal timing in a neotropical katydid an adaptive response to variation in wind-induced vibratory noise? *Behavioral Ecology and Sociobiology*, *74*(5), 59. https://doi.org/10.1007/s00265-020-02842-z

Vidal, O., & Rendón-Salinas, E. (2014). Dynamics and trends of overwintering colonies of the monarch butterfly in Mexico. *Biological Conservation*, *180*, 165–175. https://doi.org/10.1016/j.biocon.2014.09.041

Weiss, S. B. (2018, June). *Albany Hill Monarch Habitat Assessment*. Creekside Science.

Weiss, S. B., & Rich, P. M. (2008, February 1). *Recommendations for Restoration of Monarch Butterfly Winter Habitat at Norma B. Gibbs Park, Huntington Beach, CA*. Creekside Center for Earth Observation. Menlo Park, CA. http://www.creeksidescience.com

Weiss, S. B., Rich, P. M., Murphy, D. D., Calvert, W. H., & Ehrlich, P. R. (1991). Forest Canopy Structure at Overwintering Monarch Butterfly Sites: Measurements with Hemispherical Photography. *Conservation Biology*, *5*(2), 165–175. https://doi.org/10.1111/j.1523-1739.1991.tb00121.x

Xerces Society. (2016). *State of the Monarch Overwintering Sites in California* (16-015_01). The Xerces Society for Invertebrate Conservation. Portland, OR. Retrieved October 3, 2024, from https://www.xerces.org/sites/default/files/2018-05/16-015_01_XercesSoc_State-of-Monarch-Overwintering-Sites-in-California_web.pdf

Xerces Society. (2017, October). *Step-by-Step Western Monarch Thanksgiving Count Monitoring Guide*.

Xerces Society. (2018). *Managing for Monarchs in the West: Best Management Practices for Conserving the Monarch Butterfly and its Habitat*. The Xerces Society for Invertebrate Conservation. Portland, OR. www.xerces.org

Xerces Society. (2025a). *Western Monarch Thanksgiving Count and New Year's Count Data, 1997-2025*. https://westernmonarchcount.org/

Xerces Society. (2025b, March 6). *Western Monarch Butterfly Population Declines to Near Record Low*. Retrieved June 4, 2025, from https://www.xerces.org/press/western-monarch-butterfly-population-declines-to-near-record-low

Yang, L. H., Ostrovsky, D., Rogers, M. C., & Welker, J. M. (2016). Intra-population variation in the natal origins and wing morphology of overwintering western monarch butterflies *Danaus plexippus*. *Ecography*, *39*(10), 998–1007. https://doi.org/10.1111/ecog.01994

Zalucki, M. P. (1982). Temperature and Rate of Development in Danaus Plexippus L. and D. Chrysippus L. (lepidoptera:nymphalidae). *Australian Journal of Entomology*, *21*(4), 241–246. https://doi.org/10.1111/j.1440-6055.1982.tb01803.x

APPENDICES

Appendix A

30-MINUTE WIND DISRUPTION ANALYSIS: CANDIDATE MODELS

This appendix documents all candidate models tested in the 30-minute wind disruption analysis. A total of 52 models were evaluated to identify the best-fitting model for predicting short-term changes in butterfly cluster presence based on weather conditions and direct sun exposure.

A.1 Model Structure

All models used Generalized Additive Mixed Models (GAMM) with the following structure:

- **Response variable**: $\sqrt[3]{\Delta\text{Butterflies}}$ (cube root of butterfly count change between consecutive 30-minute intervals)
- **Random effects**: Random intercept for deployment site
- **Correlation structure**: AR(1) autocorrelation within observation days
- **Estimation method**: Restricted Maximum Likelihood (REML)

A.2 Variable Definitions

- `total_butterflies_t_lag`: Previous butterfly count (lagged)
- `max_gust`: Maximum wind gust speed (m/s)
- `temperature_avg`: Average temperature (°C)
- `butterflies_direct_sun_t_lag`: Butterflies in direct sun (lagged)
- `time_within_day_t`: Time since sunrise (hours)
- `s()`: Thin-plate regression spline smooth term
- `ti()`: Tensor product interaction smooth
- `*`: Linear interaction term

A.3 Candidate Models

Table A.1: *Complete list of 52 candidate models tested in 30-minute wind disruption analysis*

Model	Formula
M1	total_butterflies_t_lag
M2	total_butterflies_t_lag + max_gust
M3	total_butterflies_t_lag + temperature_avg
M4	total_butterflies_t_lag + butterflies_direct_sun_t_lag
M5	total_butterflies_t_lag + max_gust + temperature_avg
M6	total_butterflies_t_lag + max_gust + butterflies_direct_sun_t_lag
M7	total_butterflies_t_lag + temperature_avg + butterflies_direct_sun_t_lag

Continued on next page

Table A.1 – continued from previous page

Model	Formula
M8	total_butterflies_t_lag + max_gust + temperature_avg + butterflies_direct_sun_t_lag
M9	total_butterflies_t_lag + max_gust * temperature_avg
M10	total_butterflies_t_lag + max_gust * butterflies_direct_sun_t_lag
M11	total_butterflies_t_lag + temperature_avg * butterflies_direct_sun_t_lag
M12	total_butterflies_t_lag + max_gust * temperature_avg + butterflies_direct_sun_t_lag
M13	total_butterflies_t_lag + max_gust * butterflies_direct_sun_t_lag + temperature_avg
M14	total_butterflies_t_lag + temperature_avg * butterflies_direct_sun_t_lag + max_gust
M15	total_butterflies_t_lag + max_gust * temperature_avg + max_gust * butterflies_direct_sun_t_lag + temperature_avg * butterflies_direct_sun_t_lag
M16	total_butterflies_t_lag + max_gust * temperature_avg * butterflies_direct_sun_t_lag
M17	s(total_butterflies_t_lag) + s(temperature_avg) + s(butterflies_direct_sun_t_lag)
M18	s(total_butterflies_t_lag) + temperature_avg + s(butterflies_direct_sun_t_lag)
M19	s(total_butterflies_t_lag) + s(max_gust) + temperature_avg + s(butterflies_direct_sun_t_lag)
M20	s(total_butterflies_t_lag) + s(temperature_avg) + s(butterflies_direct_sun_t_lag)
M21	s(total_butterflies_t_lag) + s(max_gust) + s(temperature_avg) + s(butterflies_direct_sun_t_lag)
M22	s(total_butterflies_t_lag) + temperature_avg + s(butterflies_direct_sun_t_lag) + s(time_within_day_t)
M23	s(total_butterflies_t_lag) + s(temperature_avg) + s(butterflies_direct_sun_t_lag) + s(time_within_day_t)

Continued on next page

Table A.1 – continued from previous page

Model	Formula
M24	s(total_butterflies_t_lag) + s(max_gust) + s(temperature_avg) + s(butterflies_direct_sun_t_lag) + s(time_within_day_t)
M25	1 (intercept only)
M26	max_gust
M27	temperature_avg
M28	butterflies_direct_sun_t_lag
M29	max_gust + temperature_avg
M30	max_gust + butterflies_direct_sun_t_lag
M31	temperature_avg + butterflies_direct_sun_t_lag
M32	max_gust + temperature_avg + butterflies_direct_sun_t_lag
M33	max_gust * temperature_avg
M34	max_gust * butterflies_direct_sun_t_lag
M35	temperature_avg * butterflies_direct_sun_t_lag
M36	max_gust * temperature_avg + butterflies_direct_sun_t_lag
M37	max_gust * butterflies_direct_sun_t_lag + temperature_avg
M38	temperature_avg * butterflies_direct_sun_t_lag + max_gust
M39	max_gust * temperature_avg + max_gust * butterflies_direct_sun_t_lag + temperature_avg * butterflies_direct_sun_t_lag
M40	max_gust * temperature_avg * butterflies_direct_sun_t_lag
M41	s(temperature_avg) + s(butterflies_direct_sun_t_lag)
M42	temperature_avg + s(butterflies_direct_sun_t_lag)
M43	s(max_gust) + temperature_avg + s(butterflies_direct_sun_t_lag)
M44	s(temperature_avg) + s(butterflies_direct_sun_t_lag)
M45	s(max_gust) + s(temperature_avg) + s(butterflies_direct_sun_t_lag)
M46	temperature_avg + s(butterflies_direct_sun_t_lag) + s(time_within_day_t)
M47	s(temperature_avg) + s(butterflies_direct_sun_t_lag) + s(time_within_day_t)
M48	s(max_gust) + s(temperature_avg) + s(butterflies_direct_sun_t_lag) + s(time_within_day_t)

Continued on next page

Table A.1 – continued from previous page

Model	Formula
M49	s(total_butterflies_t_lag) + ti(max_gust, butterflies_direct_sun_t_lag)
M50	s(total_butterflies_t_lag) + s(temperature_avg) + s(time_within_day_t) + ti(max_gust, butterflies_direct_sun_t_lag)
M51	ti(max_gust, butterflies_direct_sun_t_lag)
M52	s(temperature_avg) + s(time_within_day_t) + ti(max_gust, butterflies_direct_sun_t_lag)

A.4 Model Selection Results

Model M50 was identified as the best-fit model based on Akaike Information Criterion (AIC). Complete model selection statistics and parameter estimates for the best-fit model are reported in the main text.

Appendix B

THRESHOLD WIND DISRUPTION ANALYSIS: CANDIDATE MODELS

This appendix documents all candidate models tested in the threshold wind disruption sensitivity analysis. A total of 52 models were evaluated using a binary threshold-based wind metric to compare with the continuous maximum gust approach.

B.1 Model Structure

All models used Generalized Additive Mixed Models (GAMM) with the following structure:

- **Response variable**: $\sqrt[3]{\Delta\text{Butterflies}}$ (cube root of butterfly count change between consecutive 30-minute intervals)
- **Random effects**: Random intercept for deployment site
- **Correlation structure**: AR(1) autocorrelation within observation days
- **Estimation method**: Restricted Maximum Likelihood (REML)

B.2 Variable Definitions

- `total_butterflies_t_lag`: Previous butterfly count (lagged)
- `minutes_above_threshold`: Minutes with wind speed ≥ 2 m/s
- `temperature_avg`: Average temperature (°C)

- `butterflies_direct_sun_t_lag`: Butterflies in direct sun (lagged)
- `time_within_day_t`: Time since sunrise (hours)
- `s()`: Thin-plate regression spline smooth term
- `ti()`: Tensor product interaction smooth
- `*`: Linear interaction term

B.3 Candidate Models

Table B.1: *Complete list of 52 candidate models tested in threshold wind disruption analysis*

Model	Formula
T1	total_butterflies_t_lag
T2	total_butterflies_t_lag + minutes_above_threshold
T3	total_butterflies_t_lag + temperature_avg
T4	total_butterflies_t_lag + butterflies_direct_sun_t_lag
T5	total_butterflies_t_lag + minutes_above_threshold + temperature_avg
T6	total_butterflies_t_lag + minutes_above_threshold + butterflies_direct_sun_t_lag
T7	total_butterflies_t_lag + temperature_avg + butterflies_direct_sun_t_lag
T8	total_butterflies_t_lag + minutes_above_threshold + temperature_avg + butterflies_direct_sun_t_lag
T9	total_butterflies_t_lag + minutes_above_threshold * temperature_avg
T10	total_butterflies_t_lag + minutes_above_threshold * butterflies_direct_sun_t_lag
T11	total_butterflies_t_lag + temperature_avg * butterflies_direct_sun_t_lag

Continued on next page

Table B.1 – continued from previous page

Model	Formula
T12	total_butterflies_t_lag + minutes_above_threshold * temperature_avg + butterflies_direct_sun_t_lag
T13	total_butterflies_t_lag + minutes_above_threshold * butterflies_direct_sun_t_lag + temperature_avg
T14	total_butterflies_t_lag + temperature_avg * butterflies_direct_sun_t_lag + minutes_above_threshold
T15	total_butterflies_t_lag + minutes_above_threshold * temperature_avg + minutes_above_threshold * butterflies_direct_sun_t_lag + temperature_avg * butterflies_direct_sun_t_lag
T16	total_butterflies_t_lag + minutes_above_threshold * temperature_avg * butterflies_direct_sun_t_lag
T17	s(total_butterflies_t_lag) + s(temperature_avg) + s(butterflies_direct_sun_t_lag)
T18	s(total_butterflies_t_lag) + temperature_avg + s(butterflies_direct_sun_t_lag)
T19	s(total_butterflies_t_lag) + s(minutes_above_threshold) + temperature_avg + s(butterflies_direct_sun_t_lag)
T20	s(total_butterflies_t_lag) + s(temperature_avg) + s(butterflies_direct_sun_t_lag)
T21	s(total_butterflies_t_lag) + s(minutes_above_threshold) + s(temperature_avg) + s(butterflies_direct_sun_t_lag)
T22	s(total_butterflies_t_lag) + temperature_avg + s(butterflies_direct_sun_t_lag) + s(time_within_day_t)
T23	s(total_butterflies_t_lag) + s(temperature_avg) + s(butterflies_direct_sun_t_lag) + s(time_within_day_t)
T24	s(total_butterflies_t_lag) + s(minutes_above_threshold) + s(temperature_avg) + s(butterflies_direct_sun_t_lag) + s(time_within_day_t)
T25	1 (intercept only)
T26	minutes_above_threshold

Continued on next page

Table B.1 – continued from previous page

Model	Formula
T27	temperature_avg
T28	butterflies_direct_sun_t_lag
T29	minutes_above_threshold + temperature_avg
T30	minutes_above_threshold + butterflies_direct_sun_t_lag
T31	temperature_avg + butterflies_direct_sun_t_lag
T32	minutes_above_threshold + temperature_avg + butterflies_direct_sun_t_lag
T33	minutes_above_threshold * temperature_avg
T34	minutes_above_threshold * butterflies_direct_sun_t_lag
T35	temperature_avg * butterflies_direct_sun_t_lag
T36	minutes_above_threshold * temperature_avg + butterflies_direct_sun_t_lag
T37	minutes_above_threshold * butterflies_direct_sun_t_lag + temperature_avg
T38	temperature_avg * butterflies_direct_sun_t_lag + minutes_above_threshold
T39	minutes_above_threshold * temperature_avg + minutes_above_threshold * butterflies_direct_sun_t_lag + temperature_avg * butterflies_direct_sun_t_lag
T40	minutes_above_threshold * temperature_avg * butterflies_direct_sun_t_lag
T41	s(temperature_avg) + s(butterflies_direct_sun_t_lag)
T42	temperature_avg + s(butterflies_direct_sun_t_lag)
T43	s(minutes_above_threshold) + temperature_avg + s(butterflies_direct_sun_t_lag)
T44	s(temperature_avg) + s(butterflies_direct_sun_t_lag)
T45	s(minutes_above_threshold) + s(temperature_avg) + s(butterflies_direct_sun_t_lag)
T46	temperature_avg + s(butterflies_direct_sun_t_lag) + s(time_within_day_t)
T47	s(temperature_avg) + s(butterflies_direct_sun_t_lag) + s(time_within_day_t)
T48	s(minutes_above_threshold) + s(temperature_avg) + s(butterflies_direct_sun_t_lag) + s(time_within_day_t)
T49	s(total_butterflies_t_lag) + ti(minutes_above_threshold, butterflies_direct_sun_t_lag)

Continued on next page

Table B.1 – continued from previous page

Model	Formula
T50	s(total_butterflies_t_lag) + s(temperature_avg) + s(time_within_day_t) + ti(minutes_above_threshold, butterflies_direct_sun_t_lag)
T51	ti(minutes_above_threshold, butterflies_direct_sun_t_lag)
T52	s(temperature_avg) + s(time_within_day_t) + ti(minutes_above_threshold, butterflies_direct_sun_t_lag)

B.4 Model Selection Results

Model T50 was identified as the best-fit model based on Akaike Information Criterion (AIC). This model structure mirrors M50 from the continuous wind analysis, enabling direct comparison between threshold-based and continuous wind metrics. Complete model selection statistics are reported in the main text.

Appendix C

SITE FIDELITY ANALYSIS (SUNSET WINDOW): CANDIDATE MODELS

This appendix documents all candidate models tested in the sunset window site fidelity analysis. A total of 78 models were evaluated to identify factors predicting daily changes in roost abandonment using a biologically-aligned weather window (from time of maximum count through functional sunset).

C.1 Model Structure

All models used Generalized Additive Mixed Models (GAMM) with the following structure:

- **Response variable**: $\sqrt{\Delta \text{Butterflies}_{95th}}$ (square root of change in 95th percentile butterfly count between days)
- **Random effects**: Random intercept for deployment site
- **Correlation structure**: AR(1) autocorrelation for temporal dependence
- **Estimation method**: Restricted Maximum Likelihood (REML)

C.2 Variable Definitions

- `max_butterflies_t_1`: Previous day maximum count (tested as smooth or linear)
- `lag_duration_hours`: Weather window duration (tested as smooth or linear)

- `temp_min`: Minimum temperature from max count to sunset (°C)
- `temp_max`: Maximum temperature from max count to sunset (°C)
- `temp_at_max_count_t_1`: Temperature when max count occurred (°C)
- `wind_max_gust`: Maximum wind gust in window (m/s)
- `sum_butterflies_direct_sun`: Cumulative butterflies in direct sun
- `s()`: Thin-plate regression spline smooth term
- `ti()`: Tensor product interaction smooth

C.3 Candidate Models

Models were generated programmatically across seven categories. The first number in parentheses indicates models with smooth baseline controls; the second indicates linear baseline controls.

Table C.1: *Complete list of 78 candidate models tested in sunset window site fidelity analysis*

Model	**Description**
Part 1: Null Models (2 models)	
M1	Null (smooth baseline)
M2	Null (linear baseline)
Part 2: Single Predictor Models (10 models)	
M3, M4	Single: temp_min (smooth, linear)
M5, M6	Single: temp_max (smooth, linear)
M7, M8	Single: temp_at_max_count_t_1 (smooth, linear)
M9, M10	Single: wind_max_gust (smooth, linear)

Continued on next page

Table C.1 – continued from previous page

Model	Description
M11, M12	Single: sum_butterflies_direct_sun (smooth, linear)
Part 3: Two-Way Interaction Models (20 models)	
M13, M14	Interaction: temp_min × temp_max (smooth, linear)
M15, M16	Interaction: temp_min × temp_at_max_count_t_1 (smooth, linear)
M17, M18	Interaction: temp_min × wind_max_gust (smooth, linear)
M19, M20	Interaction: temp_min × sum_butterflies_direct_sun (smooth, linear)
M21, M22	Interaction: temp_max × temp_at_max_count_t_1 (smooth, linear)
M23, M24	Interaction: temp_max × wind_max_gust (smooth, linear)
M25, M26	Interaction: temp_max × sum_butterflies_direct_sun (smooth, linear)
M27, M28	Interaction: temp_at_max_count_t_1 × wind_max_gust (smooth, linear)
M29, M30	Interaction: temp_at_max_count_t_1 × sum_butterflies_direct_sun (smooth, linear)
M31, M32	Interaction: wind_max_gust × sum_butterflies_direct_sun (smooth, linear)
Part 4: Main Effects + Interaction Models (20 models)	
M33, M34	Additive + Interaction: temp_min + temp_max + interaction (smooth, linear)
M35, M36	Additive + Interaction: temp_min + temp_at_max_count_t_1 + interaction (smooth, linear)
M37, M38	Additive + Interaction: temp_min + wind_max_gust + interaction (smooth, linear)
M39, M40	Additive + Interaction: temp_min + sum_butterflies_direct_sun + interaction (smooth, linear)
M41, M42	Additive + Interaction: temp_max + temp_at_max_count_t_1 + interaction (smooth, linear)

Continued on next page

Table C.1 – continued from previous page

Model	Description
M43, M44	Additive + Interaction: temp_max + wind_max_gust + interaction (smooth, linear)
M45, M46	Additive + Interaction: temp_max + sum_butterflies_direct_sun + interaction (smooth, linear)
M47, M48	Additive + Interaction: temp_at_max_count_t_1 + wind_max_gust + interaction (smooth, linear)
M49, M50	Additive + Interaction: temp_at_max_count_t_1 + sum_butterflies_direct_sun + interaction (smooth, linear)
M51, M52	Additive + Interaction: wind_max_gust + sum_butterflies_direct_sun + interaction (smooth, linear)
Part 5: Strategic Additive Combinations (14 models)	
M53, M54	Additive: All temperature variables (smooth, linear)
M55, M56	Additive: temp_min + temp_max (smooth, linear)
M57, M58	Additive: temp_min + wind_max_gust (smooth, linear)
M59, M60	Additive: temp_max + wind_max_gust (smooth, linear)
M61, M62	Additive: temp_at_max_count_t_1 + wind_max_gust (smooth, linear)
M63, M64	Additive: All temperature + wind (smooth, linear)
M65, M66	Additive: All predictors (smooth, linear)
Part 6: Complex Models with Multiple Interactions (6 models)	
M67, M68	All temperature main effects + all temperature interactions (smooth, linear)
M69, M70	All main effects + all temperature × wind interactions (smooth, linear)
M71, M72	FULL MODEL: All main effects + all two-way interactions (smooth, linear)
Part 7: Extra Linear Interaction Candidates (2 models)	
M77	Linear interaction: wind_max_gust × sum_butterflies_direct_sun

Continued on next page

Table C.1 – continued from previous page

Model	Description
M78	Linear interaction + temp_min + temp_max

C.4 Model Selection Results

Model M32 (Interaction: wind_max_gust × sum_butterflies_direct_sun with linear baseline) was identified as the best-fit model based on AICc (small-sample corrected AIC). Of the 78 candidate models, 42 converged successfully; models with smooth baseline controls generally failed to converge due to sample size limitations (n = 96 lag pairs). Complete model selection statistics are reported in the main text.

Appendix D

24-HOUR ROBUSTNESS ANALYSIS: CANDIDATE MODELS

This appendix documents all candidate models tested in the 24-hour robustness analysis. A total of 76 models were evaluated using a fixed 24-hour weather window to validate findings from the sunset window analysis.

D.1 Model Structure

All models used Generalized Additive Mixed Models (GAMM) with the following structure:

- **Response variable**: $\sqrt{\Delta \text{Butterflies}_{95th}}$ (square root of change in 95th percentile butterfly count between days)
- **Random effects**: Random intercept for deployment site
- **Correlation structure**: AR(1) autocorrelation for temporal dependence
- **Estimation method**: Restricted Maximum Likelihood (REML)

D.2 Variable Definitions

- `max_butterflies_t_1`: Previous day maximum count (tested as smooth or linear)
- `lag_duration_hours`: Weather window duration (24 hours, constant)

- `temp_min`: Minimum temperature in 24-hour window (°C)
- `temp_max`: Maximum temperature in 24-hour window (°C)
- `temp_at_max_count_t_1`: Temperature when max count occurred (°C)
- `wind_max_gust`: Maximum wind gust in 24-hour window (m/s)
- `sum_butterflies_direct_sun`: Cumulative butterflies in direct sun
- `s()`: Thin-plate regression spline smooth term
- `ti()`: Tensor product interaction smooth

D.3 Candidate Models

Models were generated programmatically across seven categories, identical to the sunset window analysis structure. The first number in parentheses indicates models with smooth baseline controls; the second indicates linear baseline controls.

Table D.1: *Complete list of 76 candidate models tested in 24-hour robustness analysis*

Model	**Description**
Part 1: Null Models (2 models)	
M1	Null (smooth baseline)
M2	Null (linear baseline)
Part 2: Single Predictor Models (10 models)	
M3, M4	Single: temp_min (smooth, linear)
M5, M6	Single: temp_max (smooth, linear)
M7, M8	Single: temp_at_max_count_t_1 (smooth, linear)
M9, M10	Single: wind_max_gust (smooth, linear)

Continued on next page

Table D.1 – continued from previous page

Model	Description
M11, M12	Single: sum_butterflies_direct_sun (smooth, linear)
Part 3: Two-Way Interaction Models (20 models)	
M13, M14	Interaction: temp_min × temp_max (smooth, linear)
M15, M16	Interaction: temp_min × temp_at_max_count_t_1 (smooth, linear)
M17, M18	Interaction: temp_min × wind_max_gust (smooth, linear)
M19, M20	Interaction: temp_min × sum_butterflies_direct_sun (smooth, linear)
M21, M22	Interaction: temp_max × temp_at_max_count_t_1 (smooth, linear)
M23, M24	Interaction: temp_max × wind_max_gust (smooth, linear)
M25, M26	Interaction: temp_max × sum_butterflies_direct_sun (smooth, linear)
M27, M28	Interaction: temp_at_max_count_t_1 × wind_max_gust (smooth, linear)
M29, M30	Interaction: temp_at_max_count_t_1 × sum_butterflies_direct_sun (smooth, linear)
M31, M32	Interaction: wind_max_gust × sum_butterflies_direct_sun (smooth, linear)
Part 4: Main Effects + Interaction Models (20 models)	
M33, M34	Additive + Interaction: temp_min + temp_max + interaction (smooth, linear)
M35, M36	Additive + Interaction: temp_min + temp_at_max_count_t_1 + interaction (smooth, linear)
M37, M38	Additive + Interaction: temp_min + wind_max_gust + interaction (smooth, linear)
M39, M40	Additive + Interaction: temp_min + sum_butterflies_direct_sun + interaction (smooth, linear)
M41, M42	Additive + Interaction: temp_max + temp_at_max_count_t_1 + interaction (smooth, linear)

Continued on next page

Table D.1 – continued from previous page

Model	Description
M43, M44	Additive + Interaction: temp_max + wind_max_gust + interaction (smooth, linear)
M45, M46	Additive + Interaction: temp_max + sum_butterflies_direct_sun + interaction (smooth, linear)
M47, M48	Additive + Interaction: temp_at_max_count_t_1 + wind_max_gust + interaction (smooth, linear)
M49, M50	Additive + Interaction: temp_at_max_count_t_1 + sum_butterflies_direct_sun + interaction (smooth, linear)
M51, M52	Additive + Interaction: wind_max_gust + sum_butterflies_direct_sun + interaction (smooth, linear)
Part 5: Strategic Additive Combinations (14 models)	
M53, M54	Additive: All temperature variables (smooth, linear)
M55, M56	Additive: temp_min + temp_max (smooth, linear)
M57, M58	Additive: temp_min + wind_max_gust (smooth, linear)
M59, M60	Additive: temp_max + wind_max_gust (smooth, linear)
M61, M62	Additive: temp_at_max_count_t_1 + wind_max_gust (smooth, linear)
M63, M64	Additive: All temperature + wind (smooth, linear)
M65, M66	Additive: All predictors (smooth, linear)
Part 6: Complex Models with Multiple Interactions (6 models)	
M67, M68	All temperature main effects + all temperature interactions (smooth, linear)
M69, M70	All main effects + all temperature × wind interactions (smooth, linear)
M71, M72	FULL MODEL: All main effects + all two-way interactions (smooth, linear)
Part 7: Extra Linear Interaction Candidates (4 models)	

Continued on next page

Table D.1 – continued from previous page

Model	Description
M73	Linear interaction: wind_max_gust × sum_butterflies_direct_sun (smooth baseline)
M74	Linear interaction: wind_max_gust × sum_butterflies_direct_sun (linear baseline)
M75	Linear interaction + temp_min + temp_max (smooth baseline)
M76	Linear interaction + temp_min + temp_max (linear baseline)

D.4 Model Selection Results

Model M31 (Interaction: wind_max_gust × sum_butterflies_direct_sun with smooth baseline) was identified as the best-fit model based on AICc. Of the 76 candidate models, 72 converged successfully. This analysis validated the key finding from the sunset window analysis: the interaction between wind and direct sun exposure is the strongest predictor of roost abandonment. Complete model selection statistics are reported in the main text.